JPL Publication 90-38

Design and Application of Gas-Gap Heat Switches

Final Report of Phase II

C. K. Chan
R. G. Ross, Jr.

March 15, 1990

Prepared for

Air Force Space Technology Center
Kirtland Air Force Base

Under the Sponsorship of the

Strategic Defense Initiative Organization

by

Jet Propulsion Laboratory
California Institute of Technology
Pasadena, California

JPL Publication 90-38

Design and Application of Gas-Gap Heat Switches

Final Report of Phase II

C. K. Chan
R. G. Ross, Jr.

March 15, 1990

Prepared for

Air Force Space Technology Center
Kirtland Air Force Base

Under the Sponsorship of the

Strategic Defense Initiative Organization

by

Jet Propulsion Laboratory
California Institute of Technology
Pasadena, California

ABSTRACT

Gas-gap heat switches can serve as an effective means of thermally disconnecting a standby cryocooler when the primary (operating) cooler is connected and vice versa. This report describes the final phase of the development and test of a cryogenic gas-gap heat switch designed for loads ranging from 2 watts at 8K, to 100 watts at 80K. Achieved heat-switch on/off conductance ratios ranged from 11,000 at 8K to 2200 at 80K.

A particularly challenging element of heat-switch design is achieving satisfactory operation when large temperature differentials exist across the switch. A special series of tests and analyses was conducted and used in this Phase-II activity to evaluate the developed switches for temperature differentials ranging up to 200K. Problems encountered at the maximum levels are described and analyzed, and means of avoiding the problems in the future are presented. The report concludes with a comprehensive summary of the overall heat-switch design methodology with special emphasis on lessons learned over the course of the 4-year development effort.

ACKNOWLEDGEMENTS

This publication reports the work performed under NASA Task RE-182, Amendment 403, with the Air Force Space Technology Center, Kirtland AFB, New Mexico, under the sponsorship of the Strategic Defense Initiative Organization.

The successful completion of this heat-switch development effort required important contributions from a number of individuals. Particular credit is due J. Gatewood, who fabricated the components and experimental apparatus, K. I. Boudaie, who conducted the experiments, B. Lee, who conducted the computer thermal analyses, and C. P. Kuo, who conducted the finite element structural analyses.

Dr. C. K. Chan served as manager and principal investigator from the start of the project in March 1985 until November 1988, when he left JPL to join TRW. After November 1988, Dr. Chan contributed to the final report via a JPL subcontract #958485 with TRW. Dr. R. G. Ross, Jr. managed the task following Dr. Chan's departure from JPL, including co-authoring, and publishing this final report.

Special thanks are due Dr. A. L. Johnson and J. Ligda of the Aerospace Corporation for their many comments and suggestions over the course of this development effort.

TABLE OF CONTENTS

Figures

Figures (Con't) Page

Tables

SECTION 1

INTRODUCTION

In applications where redundant cryocoolers are attached to a single load it is generally necessary to have a means of thermally disconnecting standby (nonoperating) coolers when primary units are operating, and vice versa. This disconnection is required because the parasitic heat conduction from nonoperating unit(s) is often equal to or greater than the useful cooling available from the operating unit(s).

One means of achieving the thermal disconnection function is a gas-gap heat switch. This device provides selectable thermal coupling/thermal isolation depending on the presence/absence of a conductive gas introduced in the narrow gap between the two sides of the switch. Key design parameters of a gas-gap heat switch include:

1) Achieving low radiation and conduction losses across the switch in the 'off' state.

2) Achieving high thermal conductance (low ΔT) across the switch in the 'on' state.

3) Providing for a reliable switchable source of gas (and vacuum) to the gap.

This report documents the final (second) phase of a JPL contract conducted for the Air Force Space Technology Center, Kirtland AFB, N.M., to develop a heat switch for application at temperatures ranging from 8K to 80K.

The objective of the overall contract activity, which started in 1985, was to develop and demonstrate a gas-gap heat switch with the following performance goals:

Stage	Cold Plate Temperature	Cooler Load Capability	Temperature Difference Between Cold Plate and Cold Finger
First Stage	85 K	70 to 100 watts	ΔT = 5 K
Second Stage	22 K	20 watts	ΔT = 2 K to 5 K
Third Stage	9 K	2 watts	ΔT = 1 K

1.1 SUMMARY OF THE PHASE I DEVELOPMENT EFFORT

In the first phase of the heat switch development effort a prototype heat switch was designed, analyzed, fabricated and tested over the range of cryogenic temperatures from 8K to 80K.

Figure 1-1 illustrates the Phase I heat switch design. The principal feature of the switch is the use of multiple interleaved copper fins to achieve a high surface area and narrow gas gap (0.002 inch). This maximizes thermal conduction and minimizes the temperature drop across the gap when the switch is in the 'on' state. The fins on each switch half were machined using wire electrical discharge machining (EDM), followed by hand lapping. 'Off'-state conduction losses were kept low by using a low-conduction stainless steel tube (2 inch diameter x 2 inches long x 0.004 inch thick) to support the switch halves and provide the required gas/vacuum enclosure. Operation of the switch is controlled by alternately heating or cooling a charcoal sorption bed; when the charcoal is heated, it liberates the sorbed gas into the gas gap; when it is cooled, it resorbs the gas, thus creating a vacuum in the gas gap.

Testing of the Phase I heat switch was carried out at three cryogenic temperature levels, 80K, 20K and 8K using four different working fluids: neon, nitrogen, hydrogen and helium. The 'on' conductance was measured as 5 W/K at 10K, 8 W/K at 20K, and 11 W/K at 80K. The switch ratio of 'on' conductance to 'off' conductance increased from 2200 at 80K, 7500 at 20K, to 11,000 at 10K. The major heat leaks across the switch were conduction down the stainless steel peripheral support tube, and radiation between the copper faces of the heat-switch fins.

The design methodology, mechanical drawings, and assembly process for the Phase I switch are detailed in the 183-page Phase I Final Report (Reference 1). This report also details the test apparatus, data acquisition and control procedures, and the measured results, including an error analysis. References 2 and 3 describe means of actuating the heat switch so that no electrical heater power is required.

1.2 PHASE II HEAT SWITCH DEVELOPMENT

Following the Phase I test program, a decision was made to develop and test a second (Phase II) heat switch with the objective of significantly lowering the 'off'-state parasitic conduction down the stainless steel support tube, and lowering the 'off'-state parasitic radiation between the copper fins. This led to the fabrication, test, and analysis of a Phase II prototype heat switch which incorporates low-emissivity gold-plated copper fins to reduce the radiative parasitics, and an

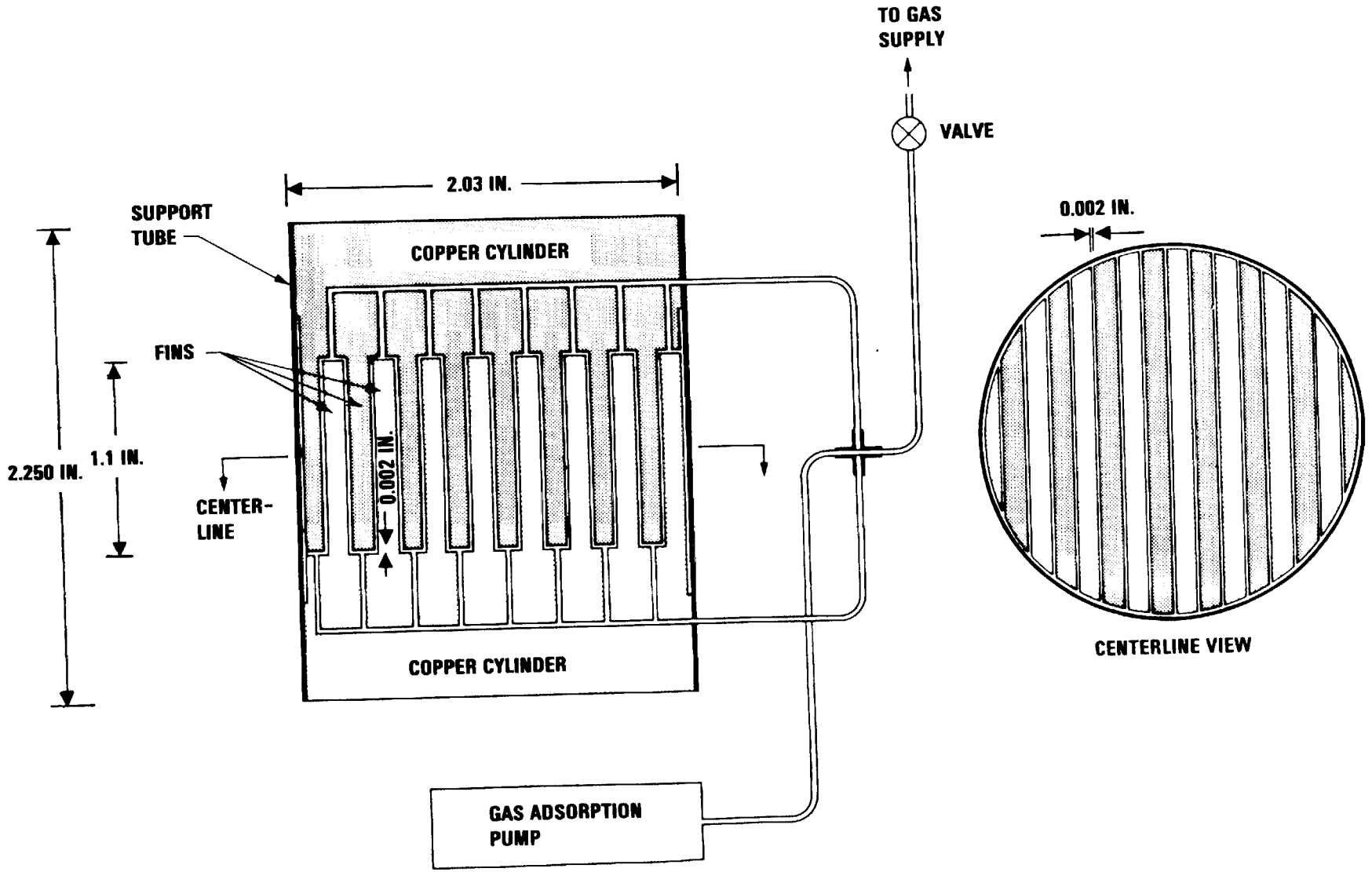

Figure 1-1. Copper Fin Heat Switch Assembly

ultra-thin-wall (0.002 inch thick) stainless steel support tube to reduce the conductive parasitics.

The design and tests conducted to characterize the performance of this gold-plated heat switch are described in this report starting in Section 2.

An area of particular importance to heat switch design is the performance of the switch under 'off'-state conditions, where one side of the switch is at cryogenic temperatures, and the other side of the switch is at the spacecraft heat rejection temperature (typically 280 to 300K). The resulting large temperature difference not only creates a large driving force for parasitic losses, but is also likely to cause highly stressful differential thermal expansion between the heat-switch halves. If not properly accommodated, this differential expansion can lead to destructive forces and/or relative motion, contacting, and thermal shorting between the switch halves. Section 3 of this report explores the details of these effects for both the Phase I and Phase II (gold-plated) heat switch design. The predictive methodology developed includes finite-element codes to predict the conductive and radiative transfer among the fins, the temperature profile on the support tube, and the associated thermal deformation.

1.3 HEAT SWITCH DESIGN GENERALIZATION

Following completion of the Phase II analysis and testing activity, a final Phase II activity was carried out to document the lessons learned in the form of guidelines for designing gas-gap heat switches for other applications. Because of the rapidly increasing interest in 60 to 80K Stirling-cycle coolers, a 1 watt cooler of this type was chosen as a design example to aid in generalizing the developed heat-switch concept. The results of this effort are presented in Section 4.

SECTION 2

PHASE II HEAT SWITCH DEVELOPMENT AND TESTING

2.1 DESIGN AND HARDWARE CONSTRUCTION

The design of the Phase II gold-plated heat switch (as shown in Figure 2-1) is fundamentally the same as the Phase I heat switch illustrated in Figure 1-1, except for several modifications for improved performance and ease of manufacturing. These include:

1) All fin surfaces were electroplated with low-emissivity gold to minimize radiant heat transfer between the hot and cold sides of the switch.

2) The thickness of the circumferential stainless steel tube was reduced from 0.004 inch to 0.002 inch, thereby reducing conductive heat transfer by a factor of two. Reducing the thickness necessitated adding three circumferential stiffening ribs to prevent the tube from collapsing under ambient external pressures.

3) The longitudinal clearance between the fin tips and the slot bottoms in the mating half was increased from 0.002 inch to 0.005 inch; this was done to preclude possible contact due to differential expansion of the stainless-steel tube versus the copper fins.

4) The actuation gas was plumbed only to the hot side of the switch to minimize parasitics to the cold side, and to simplify construction.

5) The fins were machined using a carbide circular saw instead of EDM, followed by hand lapping to achieve the precise (0.002 inch) gap dimensions; the fins were then hand polished with MET-ALL prior to gold plating.

Photographs of the disassembled and completed heat switch are shown in Figures 2-2 and 2-3, respectively.

2.2 LOW TEMPERATURE TESTS

Using the test apparatus and the procedure as outlined in Reference 1, the gold-plated heat switch was tested at liquid helium temperatures (4.2K) in both the 'on' state and 'off' state. Figure 2-4 displays the 'on'-state data for the Phase II gold-plated heat switch in comparison with that for the Phase I copper heat switch. Data are presented for two gas fill conditions: 1) 1 atm helium from an external bottle, noted as

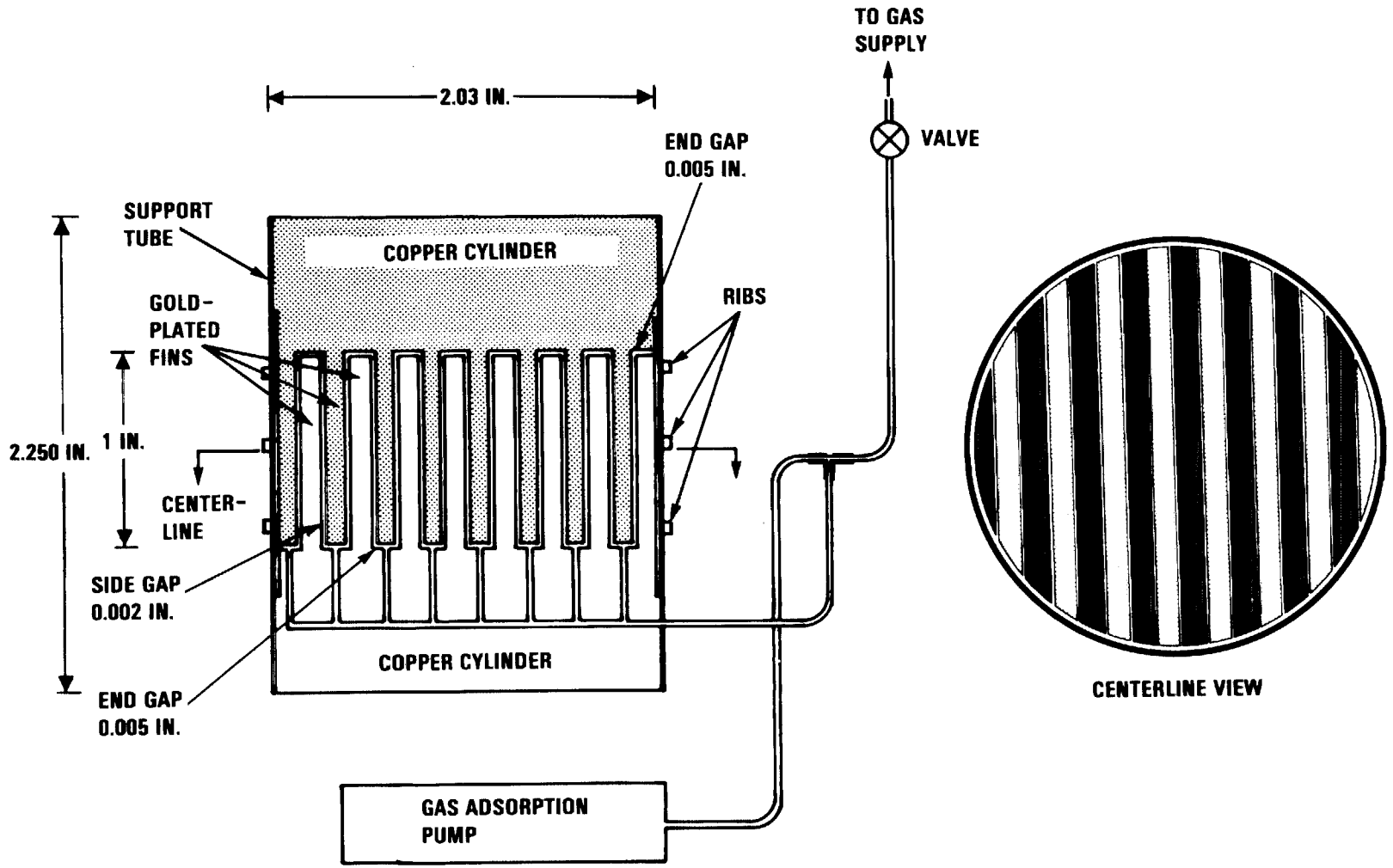

Figure 2-1. Gold-Plated Heat Switch Assembly

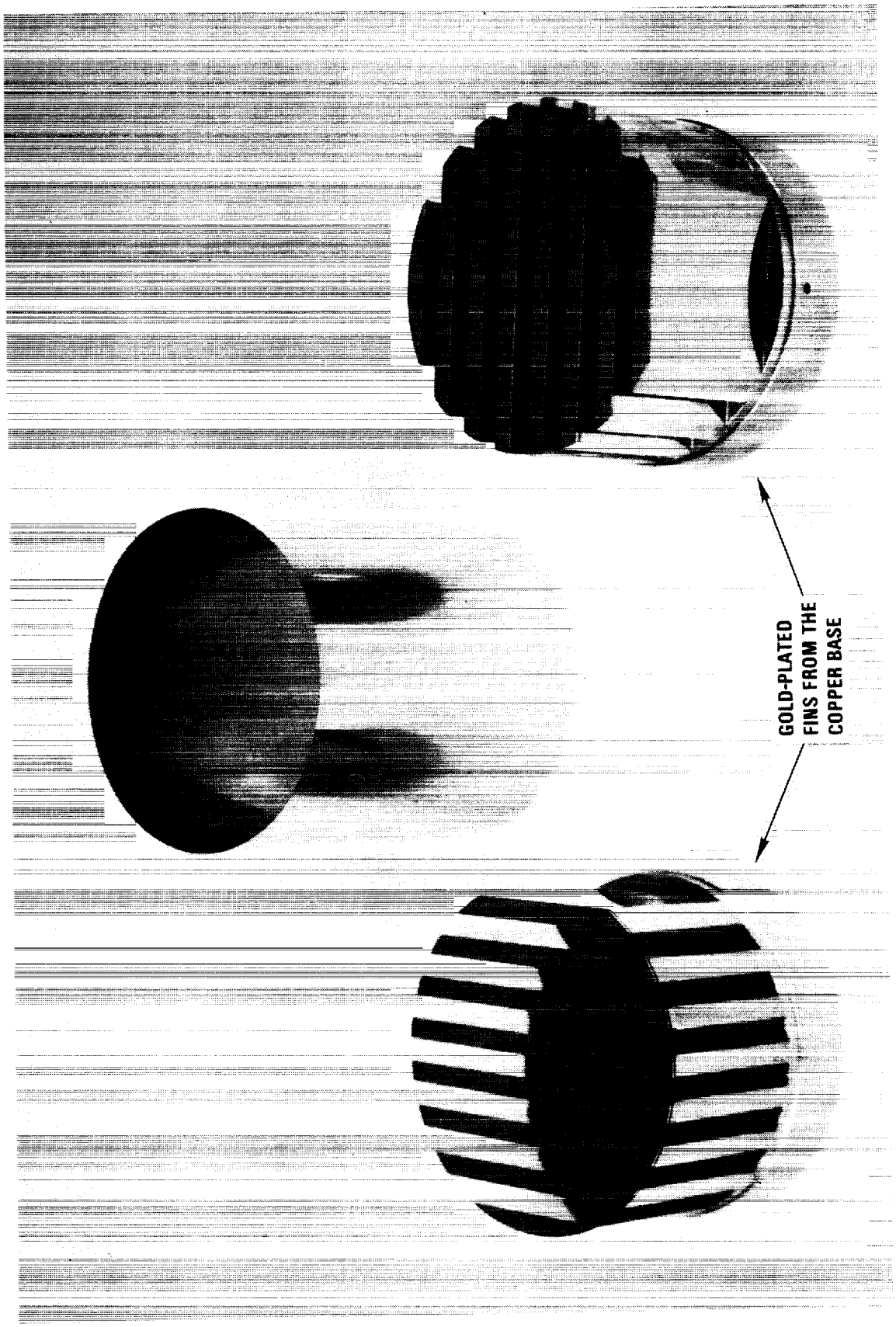

Figure 2-2. Components of Gold-Plated Heat Switch

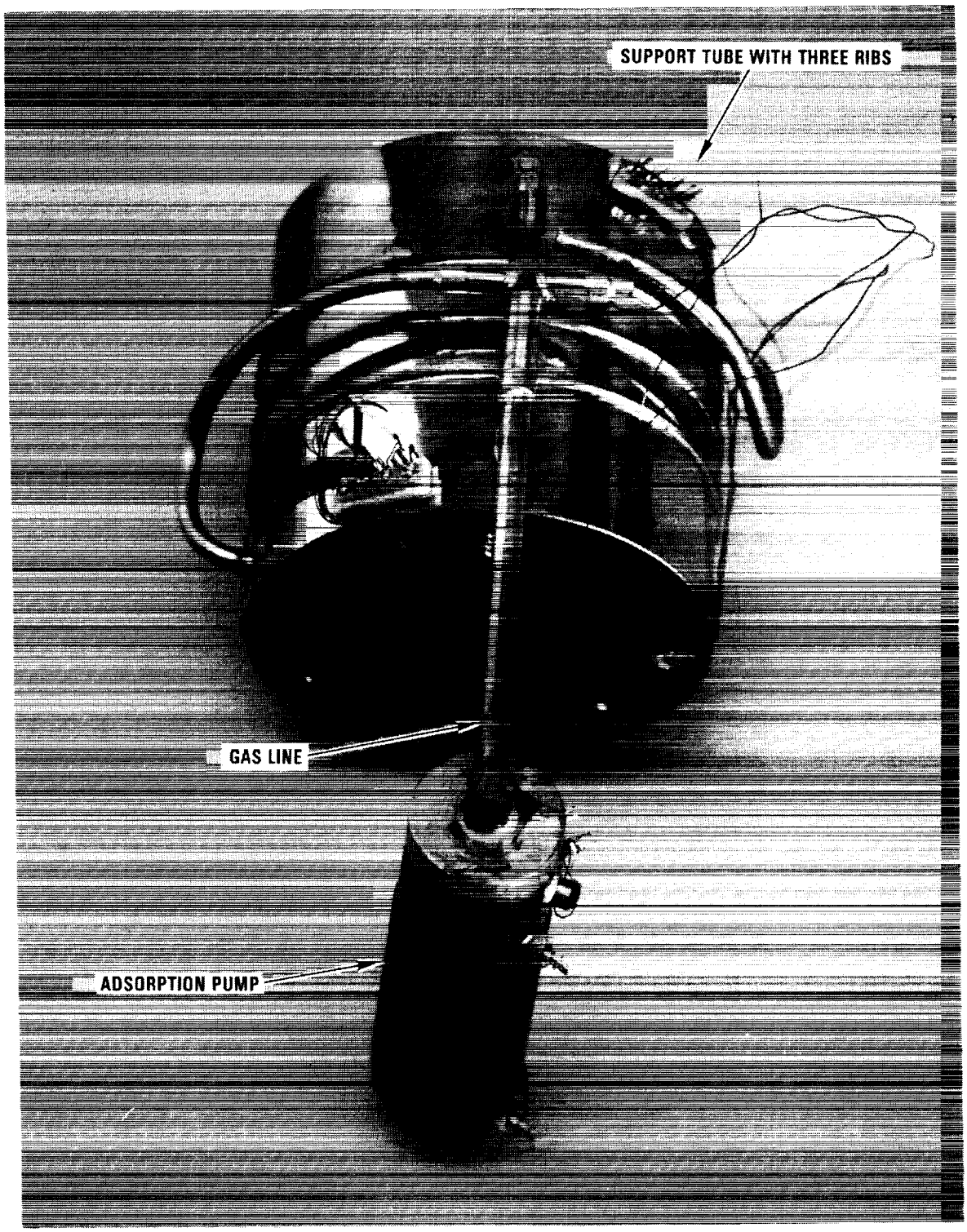

Figure 2-3. Support Tube with Three Ribs

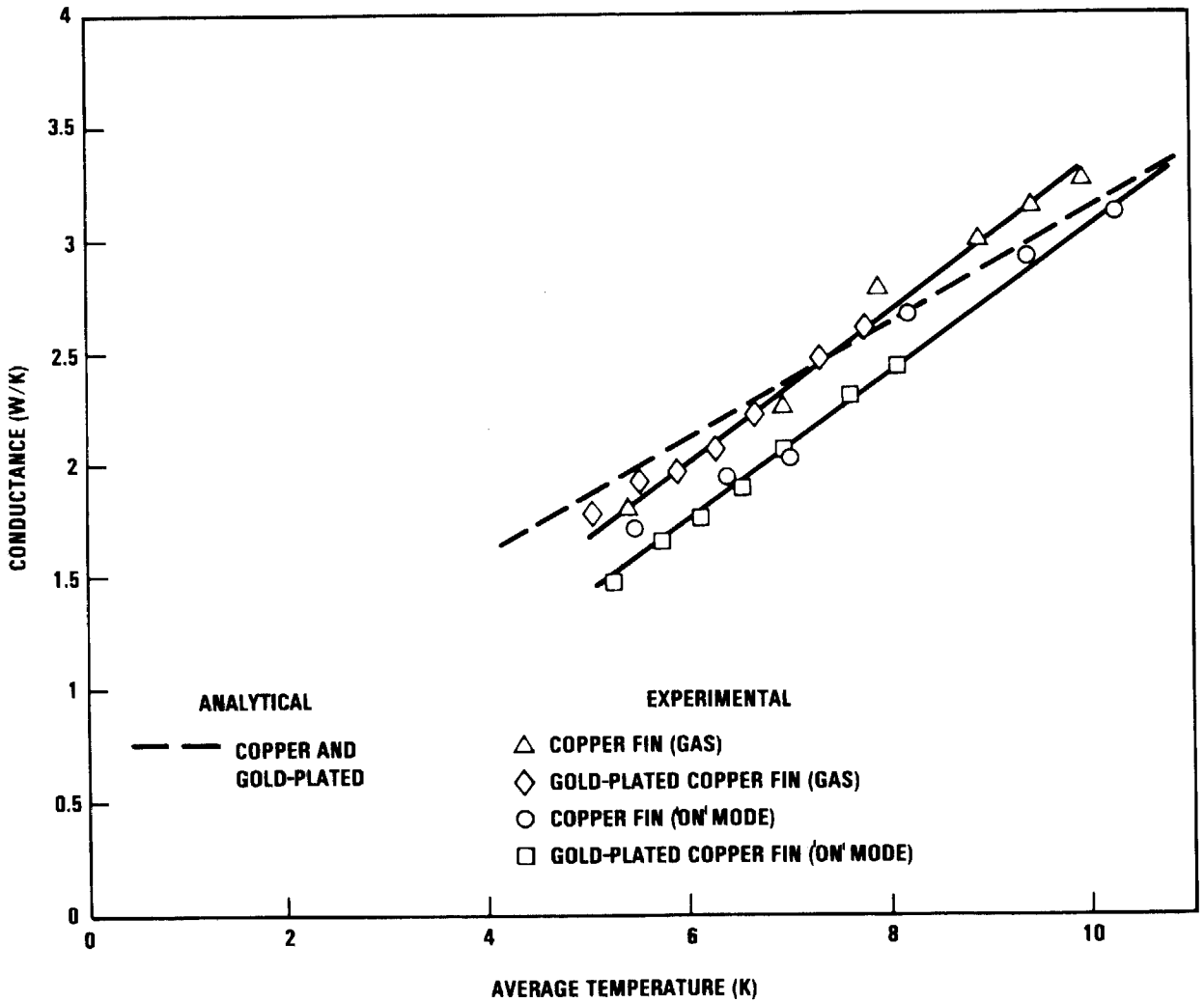

Figure 2-4. Analytical and Experimental Conductance of Copper and Gold-Plated Heat Switches When (1) Gaps are Filled with Gas at 1 atm (gas), (2) Gas is Supplied from the Gas Adsorption Pump ('on' mode) with the Temperature at the Cold End at 4.2 K

'gas', and 2) helium supplied by the sorption pump, noted as 'on mode'. As expected, little difference is seen between the 'on' performance of the Phase I and Phase II heat switches.

Figure 2-5 presents a similar comparison of the 'off'-mode performance of the two heat-switch designs--this time for two vacuum conditions: 1) vacuum provided by an external vacuum pump, referred to as 'no gas', and 2) vacuum created by the sorption pump, referred to as 'off mode'. In these tests the temperature differential across the switch was varied in the range from 4 to 16K, giving rise to average switch temperatures in the range of 6 to 10K. At these low temperatures, radiation exchange is negligible, and the primary contributor to the parasitic conductance is the thin-wall stainless-steel tube that connects the two switch halves. It can be seen from Figure 2-5 that the Phase-II gold-plated switch design, which has a 0.002-inch thick tube, has approximately one half the losses of the earlier Phase I design, which had a 0.004-inch thick tube.

Table 2-1 summarizes the performance of the two switches for the condition when the cold-side temperature is 4.2 K and the hot-side temperature is 11.8 K, i.e. the ΔT is 8 K.

2.3 TESTS WITH LARGE TEMPERATURE DIFFERENTIALS

In many applications it is foreseeable that the hot side of the heat switch will reach temperatures considerably above the cold side, and in the limit will approach a spacecraft ambient temperature near 300K. Such large temperature differentials across the heat switch not only create large driving forces for parasitic conduction and radiation to the cold side, but also cause severe differential expansion between the switch halves. Dealing with large temperature differentials thus represents one of the more difficult challenges for the heat-switch design.

A special series of tests was developed and conducted to evaluate the large-temperature-differential performance of the heat switches. In these tests the cold end of the heat switch was grounded to an 80K cold plate, while the hot end was heated with electrical resistance heaters to temperatures ranging from 90K to 270K.

In the tests, the heat flow through the heat switch was computed from the power applied to the hot-side heaters, with corrections made for parasitic losses directly to the test environment. To minimize the external losses the heat switch was outfitted with an actively controlled radiation shield as shown in Figure 2-6. One end of the shield was thermally grounded to the 80K sink, while the other end of the shield was matched to the temperature of the switch hot-side using electrical resistance guard heaters.

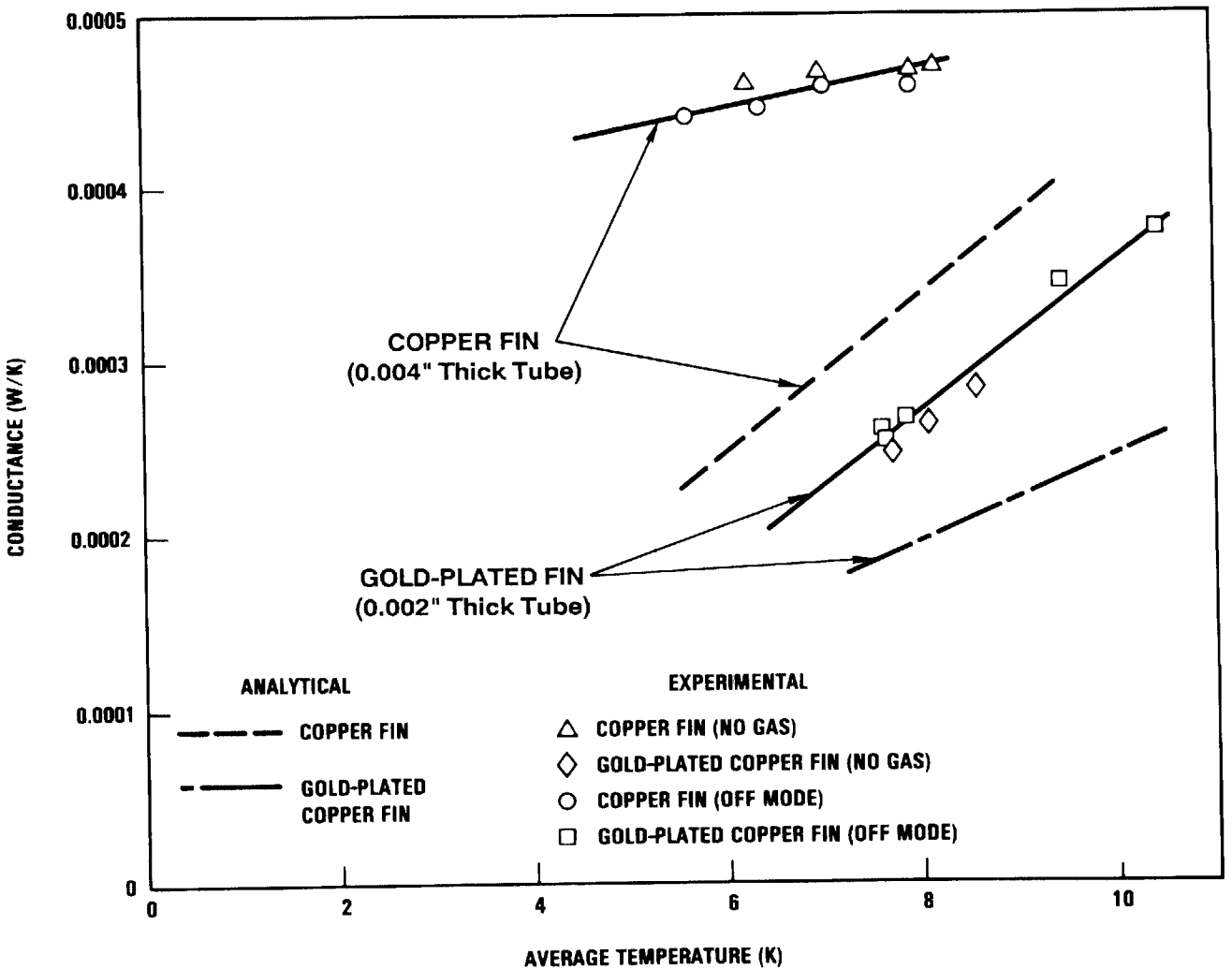

Figure 2-5. Analytical and Experimental Conductance of Copper and Gold-Plated Heat Switches When (1) Gaps are Pumped Out (no gas), (2) Gas is Removed by the Gas Adsorption Pump ('off' mode) with the Temperature at the Cold End at 4.2 K

Table 2-1. Comparison of 'On' and 'Off' Conductance and Switch Ratio for the Copper and Gold-Plated Heat Switches with a cold-side temperature of 4.2 K and a hot-side temperature of 11.8 K

AVERAGE	COPPER FIN		GOLD-PLATED FIN	
TEMPERATURE = 8K	EXPERIMENTAL	ANALYTICAL	EXPERIMENTAL	ANALYTICAL
ON CONDUCTANCE (W/K)	2.5	2.7	2.5	2.7
OFF CONDUCTANCE (W/K)	0.00047	0.00033	0.00027	0.00019
SWITCH RATIO	5300	8200	9300	14,200

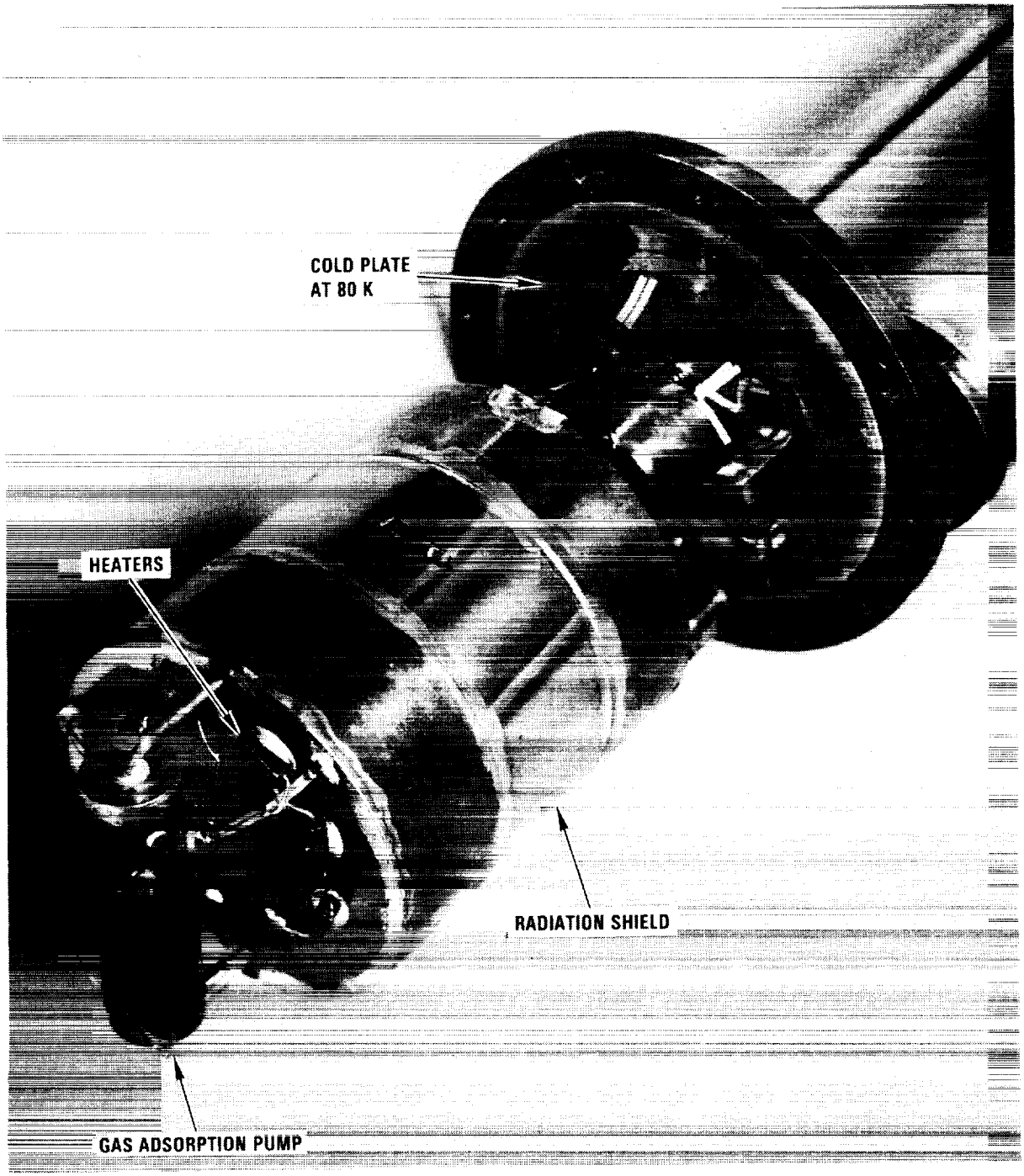

Figure 2-6. Photo of Heat Switch Test Apparatus

Figure 2-7 shows the results for the shielded and nonshielded cases. As the temperature difference between the hot and the cold base increased, the heat loss from the outer wall of the support tube to the surrounding cold dewar wall increased, as evidenced by the difference between the two curves in Figure 2-7. Figure 2-8 contrasts the performance of the earlier Phase I copper switch with that of the Phase II gold-plated switch (both without the radiation shield).

In all of the curves, it is evident that the heat flow through the heat switch abruptly increases when the temperature difference exceeds 130 to 170K. This rapid increase in heat flow suggests a mechanical breakdown in the heat switch insulation -- most likely contact between the heat switch halves caused by the significant differential expansion between the hot and cold sides.

In order to determine whether this rapid increase in heat flow was caused by contact between the cold-side fins and the hot-side fins, a series of tests that involved electrical resistance measurements was performed. The voltage (V) across the switch was measured while an electrical current (I = 1 A) was passed from the hot base to the cold base; the resistance was determined as R = V/I.

The theoretical electrical resistance of the stainless steel tube R_t is given by:

$$R_t = \rho L / \pi D t \qquad (2.1)$$

where

ρ = electrical resistivity of SS 302 (ohm-cm)
L = length of the support tube (cm)
D = diameter of the support tube (cm)
t = thickness of the support tube (cm)

In carrying out the measurements, the heat switches were first filled with 120 torr of helium gas. The resistances of both heat switches (copper and gold plated) were then measured as the hot and cold sides of the switch were cooled from room temperature to 80K. The measured resistances were found to be close to the resistance of the stainless-steel tube given by Eq.(2.1), indicating there was no touching when the hot and the cold sides were at the same temperature, i.e., no temperature differential.

Next, the heat switch was evacuated to 10^{-6} torr at room temperature. After both the hot and cold sides were cooled to equilibrium (80K), heat was applied to the hot side to raise its

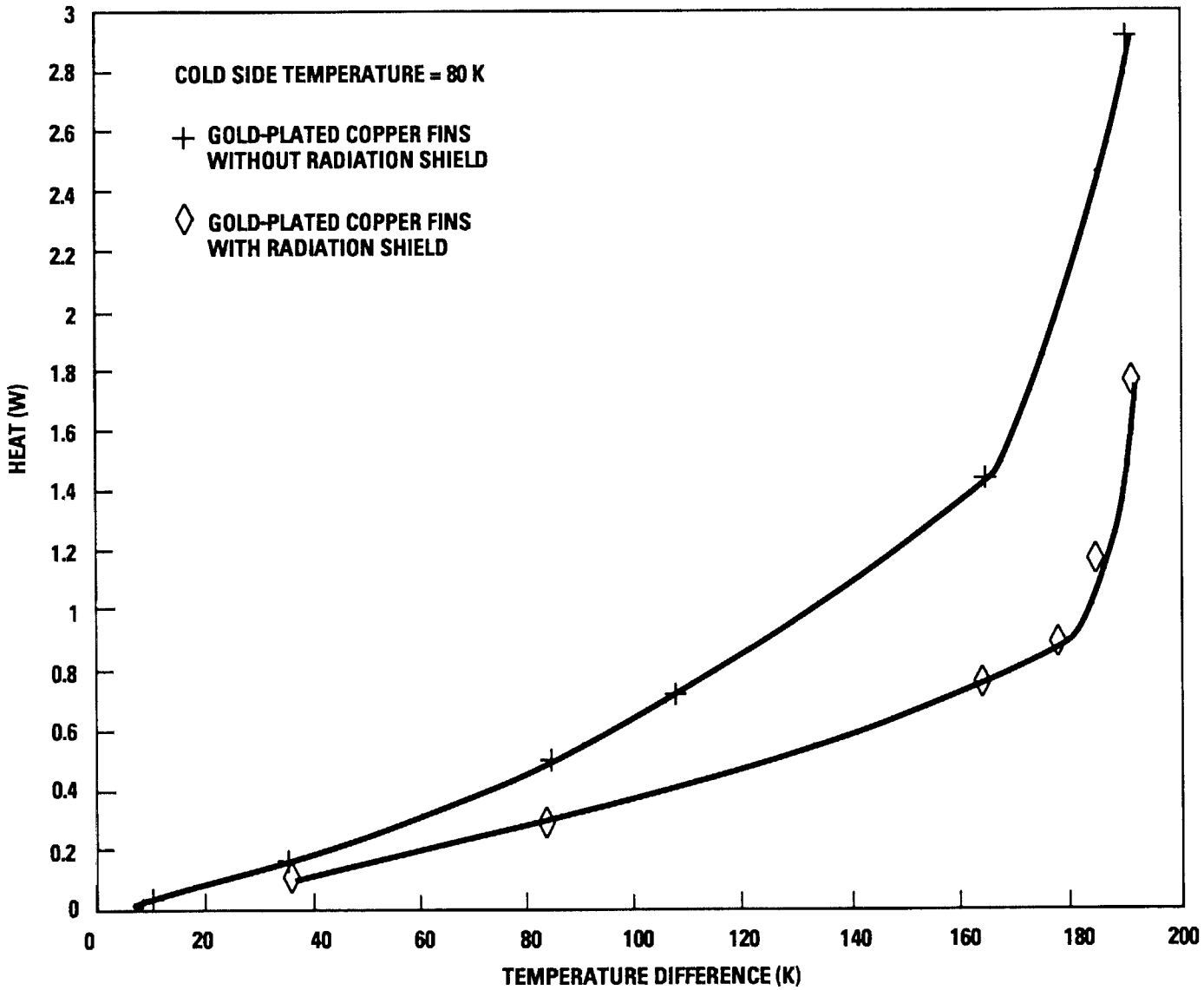

Figure 2-7. Heat Conduction of the Gold-Plated Heat Switch in the 'Off' Mode With and Without the External Radiation Shield

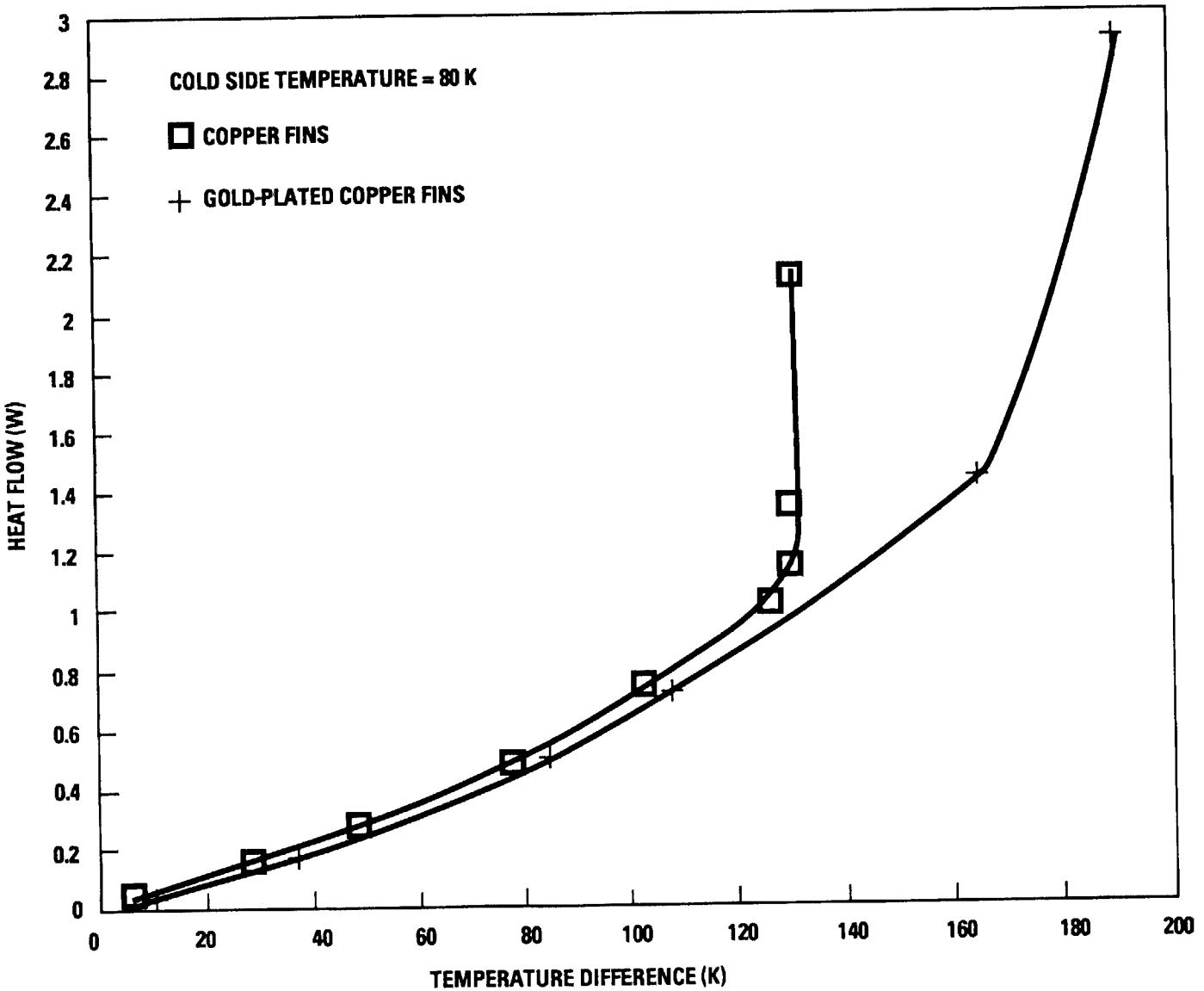

Figure 2-8. Comparison of the Heat Conduction of the Gold-Plated and Copper Heat Switches in the 'Off' Mode With No External Radiation Shield

temperature. The electrical resistance was measured at each temperature difference level (T_{hot} - T_{cold}), where T_{cold} was always 80K. For a given T_{hot} and T_{cold}, the average temperature is (T_{hot} + T_{cold})/2.

Figure 2-9 displays the measured resistances as a function of both average temperature (bottom scale) and temperature difference (top scale).

For the copper heat switch, the resistance dropped dramatically at a temperature difference of 130K, indicating that the fins did touch when the hot side temperature reached 210K (i.e., 80K + 130K). This is consistent with the results from the heat transfer test (Figure 2-8). For the tests that involved the gold-plated heat switch, the resistance decreased less abruptly, and was therefore less conclusive.

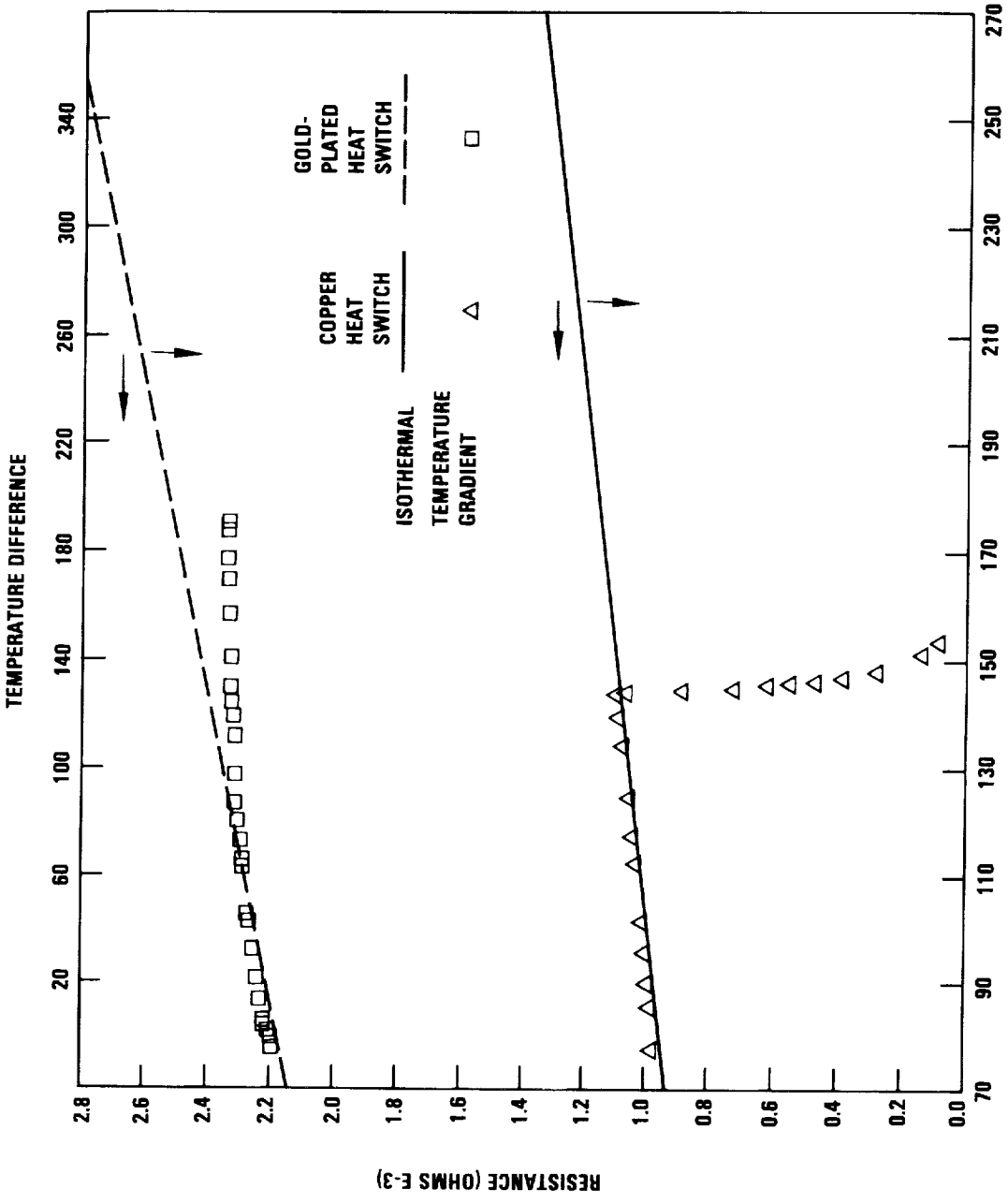

Figure 2-9. Electrical Resistance of Heat Switches

SECTION 3

ANALYSES OF PERFORMANCE LIMITATIONS CAUSED BY LARGE TEMPERATURE DIFFERENTIALS

As discussed in Section 2, the copper heat switch experienced a thermal short at a temperature difference of 130K, while the gold-plated heat switch experienced a much less severe, but similar problem, at a somewhat higher temperature. The most likely cause of this shorting is the severe differential thermal expansion that must occur between the switch sides under these conditions of large temperature difference. This Section analyzes the various differential expansion mechanisms that come into play with the subject heat switch design; specifically, the mechanisms are divided into three categories:

1) Axial expansion differences between the outer stainless-steel tube and the copper fins.

2) Radial expansion differences between the hot and cold copper-fin halves.

3) Thermal warping (bending) of the switch due to asymmetrical thermal gradients around the switch circumference.

3.1 AXIAL EXPANSION DIFFERENCES

When the heat switch operates under isothermal conditions all elements of the switch shrink according to their respective coefficients of thermal expansion (CTE) as the switch temperature is reduced below room temperature. Because copper has a higher CTE than stainless steel, the axial gap at the end of the fins actually increases as the switch cools isothermally.

In contrast, if the hot side of the switch remains at room temperature (T_R) while the cold side is reduced to a cryogenic temperature (T_C), the stainless-steel tube, of active length (L), shrinks by an amount:

$$\Delta L/L \approx CTE\ (T_R - T_C)/2 \qquad (3.1)$$

Because the hot fins do not shrink at all, a possible axial interference develops between the tips of the hot fins and the adjacent cold side of the switch. Sufficient axial clearance must be provided to preclude this possibility.

Possible axial clearance problems in the Phase I design were dealt with in the Phase II gold-plated design by increasing the fin axial clearance from the original 0.002 inch, to 0.005 inch in the Phase II design. This is very likely the reason that the Phase II design performed much better in the large-differential-temperature tests.

3.2 RADIAL EXPANSION DIFFERENCES

As with the axial dimensions of the switch, the radial, or diameter dimension of the switch also changes (shrinks) as the switch is isothermally cooled to cryogenic temperatures. Because the two switch halves are both made of copper, the shrinkage is identical and the fin alignment (spacing) remains matched for the two switch sides.

However, under conditions where the hot side remains at room temperature (T_R) and the cold side is reduced to a cryogenic temperature (T_C), the cold side will shrink radially relative to the hot side. This results in the fins on the cold side being spaced closer together than those on the hot side, a situation that can cause hot and cold fins farthest from the switch centerline to contact one another.

For this situation the change in the fin gap spacing (Δg) is given by:

$$\Delta g = CTE_{copper} \times r \times (T_R - T_C) \qquad (3.2)$$

where r is the radial distance to the gap from the switch centerline. For copper, Eq.(3.2) gives a gap closure of approximately 0.0023 inch for a temperature differential across the switch of about 170K. This correlates very well with the onset of degraded performance with the gold-plated heat switch at large temperature differentials.

3.3 THERMAL WARPING

Although the axial and radial differential expansion issues are relatively easy to understand and compute, the third category of temperature induced misalignment, thermal warpage, is highly complex. The fundamental phenomenon that can cause warpage is an asymmetrical temperature distribution around the circumference of the stainless-steel tube.

With an isothermal heat switch there are no thermal gradients, and thus there are no differential-expansion induced warpage

forces. However, with a large temperature differential across the heat switch, radiation exchange between the stainless-steel support tube and the adjacent heat-switch fins may cause the local tube temperature to partially track the adjacent fin temperature. Referring to Figure 3-1, this will cause the Fin#1 side of the support tube to run somewhat cooler than the Fin#16 side, and thus the Fin#1 side will be slightly shorter than the Fin#16 side. This will cause the switch to curl or warp toward the Fin#1 side. Had the layout of the fins been symmetrical, with, for example, a hot (or cold) fin for the outer fin on both sides, then the differential expansion forces would have been balanced, and no net warpage forces would remain.

Lacking the present state of understanding, the Phase I and Phase II heat switches were manufactured asymmetrical. To assess the degree of warpage with this design required a complex finite-difference thermal analysis to predict the tube temperature distribution, followed by a finite-element structural analysis to predict the resulting deflections.

Circumferential Temperature Distribution Analysis

Important assumptions used in the thermal analysis included:

(1) Radiation is transferred from the curved side of each fin to the inner wall of the tube.

(2) There is no heat loss from the outer wall of the tube to the surrounding environment.

(3) Heat is conducted longitudinally and circumferentially in the tube.

(4) The fins are at the same temperature as their base.

(5) The thermal conductivity of the residual helium in the gap between the wall and the fins is given by the free molecular value at 10^{-6} torr pressure.

(6) The thermal conductivity for the stainless-steel tube is temperature dependent.

Using side-to-side symmetry, only half of the cylindrical tube needed to be considered. In the model, the half-circle of the tube was modeled as a rectangular sheet of 2.54 cm height by 7.98 cm width (i.e., half the circumference). The grid points were 0.16 cm apart vertically and 0.285 cm apart horizontally. Excluding points on the isothermal boundaries where the tube was soldered to the hot and the cold copper base, there were 15 x 28 grid points. The combined gas conduction and radiation across

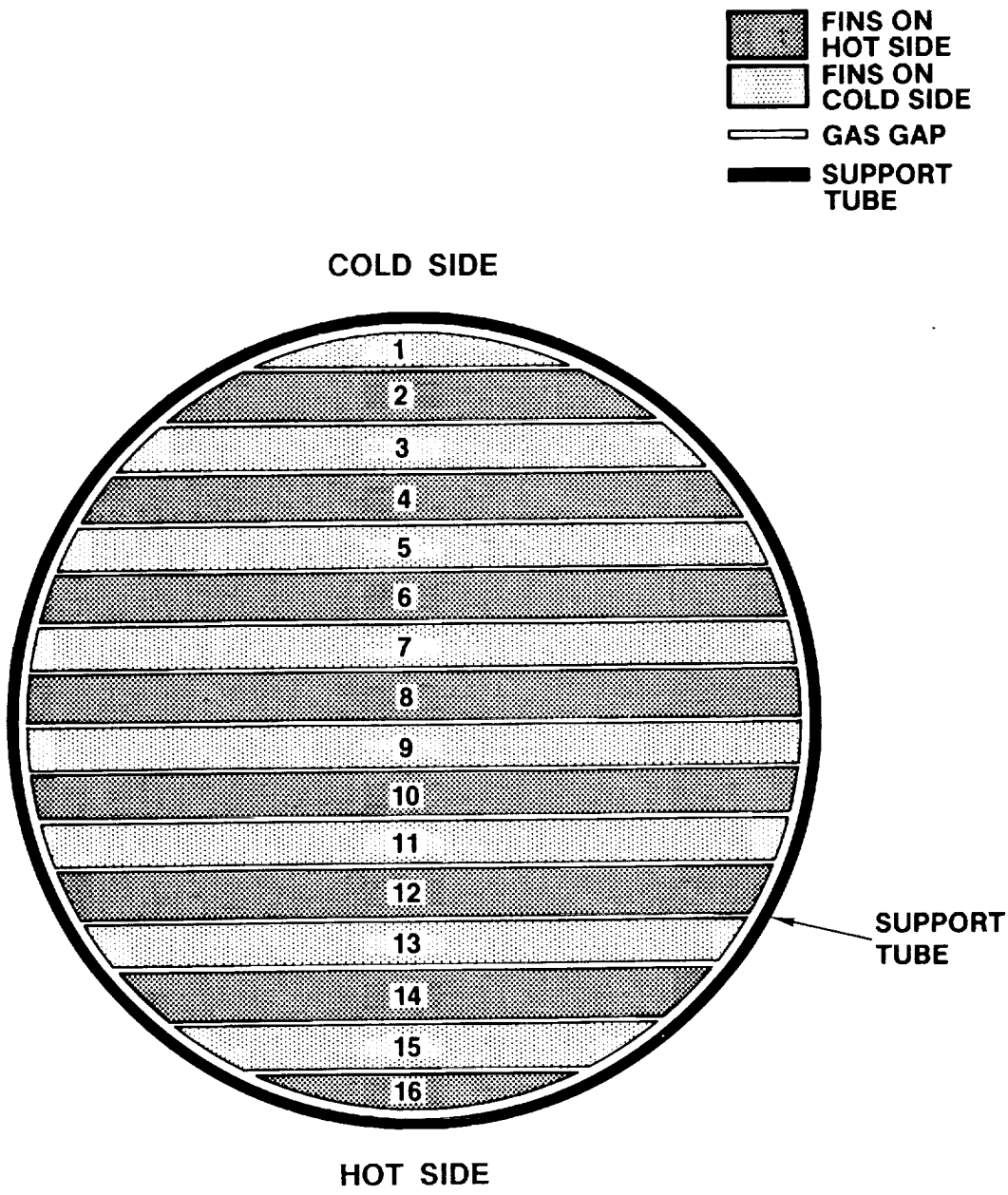

Figure 3-1. Asymmetrical Fin Arrangement of the Phase I and Phase II Heat Switches

the gap between an element on the tube and the opposing fin is given by:

$$Q = h A_g \Delta T \tag{3.3}$$

where

$h = K_g + \sigma \epsilon (T_1 + T_2)(T_1^2 + T_2^2)$
K_g = thermal conductance of He at 10^{-6} torr (watts/cm^{2}K)
σ = Stefan-Boltzmann constant (5.67×10^{-12} watts/cm^{2}K^4)
ϵ = effective emissivity, including shape factor
T_1, T_2 = temperatures of element 1 and fin 2, respectively (K)
$\Delta T = T_1 - T_2$
A_g = element gas-gap area (cm^2)

The conductive heat transfer between the support tube elements is given by:

$$Q = -k_{ss} A \nabla T \tag{3.4}$$

where

k_{ss} = thermal conductivity of stainless steel (watts/cm-K)
A = cross-sectional area of the element (cm^2)
∇T = temperature gradient (K/cm)

At steady state for each element, since no heat is accumulated, the heat transferred to and from the fins has to be transferred to the neighboring support-tube elements by conduction, both longitudinally and circumferentially. Starting from an initial guess of a linear temperature profile in the Z direction, the two-dimensional temperature profile on the tube was calculated by iteration using the relaxation method.

Deformation and Stress Analysis

To compute the deformation and stress associated with the complex temperature distribution in the support tube required a modestly complex finite-element structural analysis. In such an analysis the structure is represented by a number of small elements, each linked at their corners. The deformation at each node, i.e., the corner of each element, is calculated from a set of linear algebraic equations.

In modeling the heat switch, the relatively massive and rigid cold and hot ends were simulated as solid elements. In contrast, the support tube behaves as a flexible thin shell and was modeled using shell elements. The support tubes of both the Phase I and Phase II heat switches were investigated: the 0.004-inch tube, and the 0.002-inch tube with additional reinforcing ribs. The heat-switch fins were treated as isothermal elements rigidly attached to either the cold or the hot base. They were modeled as beam elements to accommodate the thermal expansion of the base. The total model consisted of 485 grid nodes, 16 beam elements, 44 solid elements, and 396 plate elements. A perspective view of the model is shown in Figure 3-2a.

The first step in using the model was to compute the structural deformation due only to the tube temperature distributions. These results are shown in Figure 3-2b. To get the total deformation, it is necessary to add the additional contribution resulting from the gas pressure loading, assuming 1 atm pressure outside of the tube, and vacuum inside. This is shown in Figures 3-2c and 3-2d. The addition of the gas loading turned out to be negligible, and can be safely neglected in the gap movement calculations.

Because of the nature of the tube's support, the thermal deformation of the heat switch is dependent only on the temperature distribution within the support tube, and independent of the tube thickness. Since the thermal gradients were very similar for the Phase I and Phase II switches, the relative movement at the base of the cold fin with respect to the tip of the hot fin was found to be the same for both heat-switch designs.

Figure 3-3 summarizes the computed fin displacements for each of the 15 gaps. Positive values refer to closing of the gap, and negative values refer to opening of the gap (in thousandths of an inch). The normal gap size is 0.002 inch. The calculation shows that these relative movements cause at least 3 of the 15 gaps to be closed when the temperature difference is 220K. The contact area and the contact force for this type of mechanism are much smaller than those caused by axial contraction. This may be the reason why the gold-plated heat switch experienced a much less severe contact problem than the Phase I design.

Because of the completeness of the structural analysis, the numbers shown in Figure 3-3 not only include the deformation caused by warpage, but also include that caused by the differential radial expansion discussed in the previous Section 3.2. The symmetry of the numbers about the heat-switch centerline implies that the principal deformation is, in fact, radial differential expansion; contributions from warpage appear to be quite small. However, to preclude any possible warpage problems, future heat-switch designs should adopt a symmetrical fin configuration.

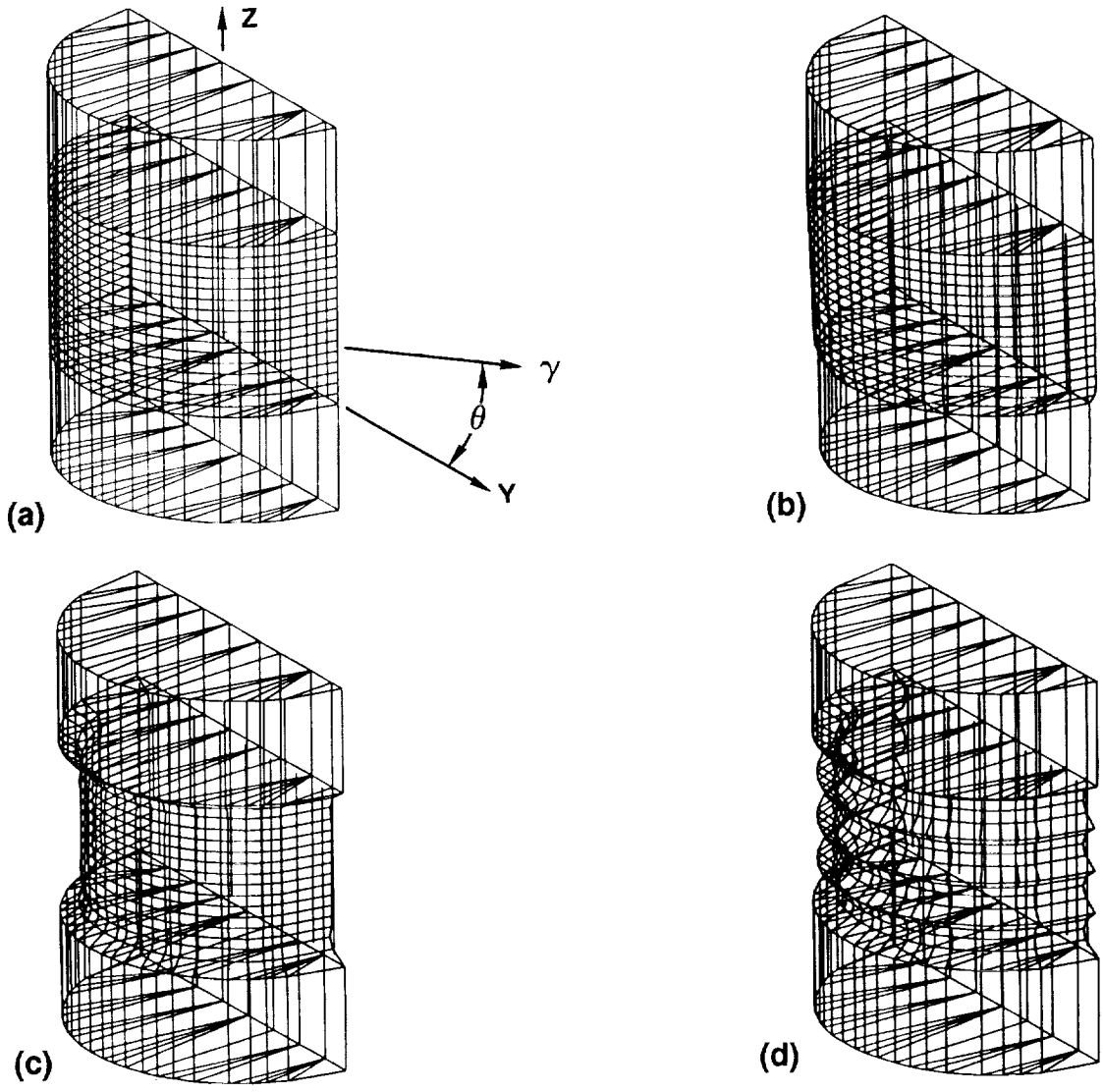

Figure 3-2. Deformation Pattern Under (a) No Stress, b) Thermal Gradient, (c) Atmospheric Pressure for 0.004 inch Wall, (d) Atmospheric Pressure for 0.002 inch Wall

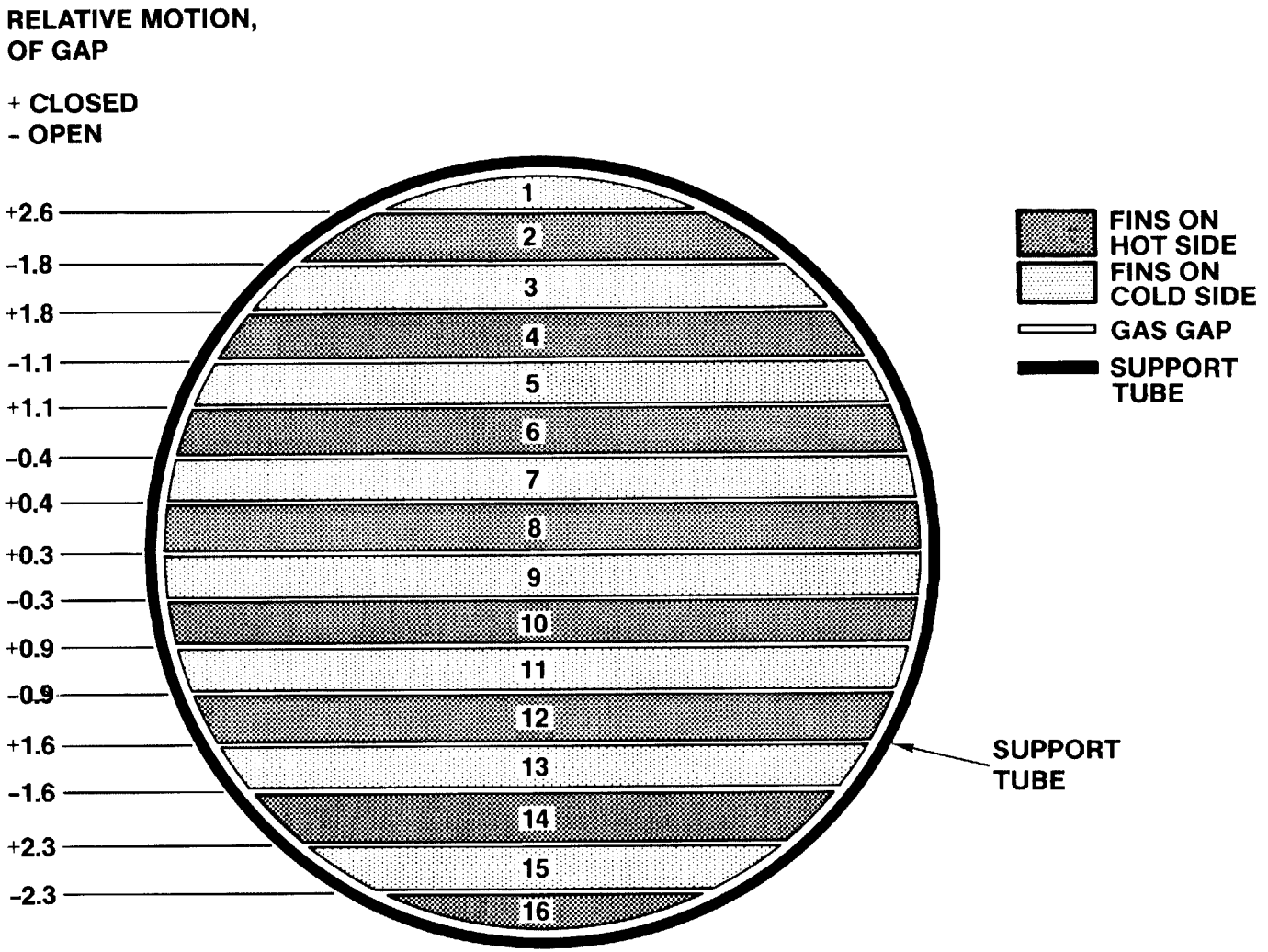

Figure 3-3. Relative Gap Motion (in 10^{-3} inch) Due to a Temperature Difference of 220 K Across the Switch

SECTION 4

HEAT SWITCH DESIGN GUIDELINES

As described earlier, the function of the gas-gap heat switch considered in this report is to provide a means of thermally disconnecting a standby (nonoperating) cooler from the cooler load when the primary (operating) cooler is connected, and vice versa. This disconnection is commonly required because the parasitic heat conduction from the nonoperating cooler may represent a significant fraction of the useful cooling available from the operating cooler (References 4,5).

The 183-page Phase I Final Report (Reference 1) provides a thorough discussion of the principles behind the operation of the gas-gap heat switch, and presents detailed data on the design tradeoffs leading to the Phase I design. Although simple in concept, cryogenic gas-gap heat switches must contend with substantial thermal gradients and widely varying material properties as the cold side of the switch is required to perform at lower and lower temperatures. The Phase I and Phase II efforts developed and used detailed computer programs that use temperature-dependent material properties to analyze the various performance attributes of gas-gap heat switches at applications as cold as 5 K.

As a complement, this section concisely summarizes the key elements in the design of cryogenic gas-gap heat switches and emphasizes lessons learned and simple calculational procedures that can quickly scope out a useful heat-switch design. Keeping the analyses simple also provides insights into the controlling parameters that are often lost in more complex numerical solutions.

By way of example, the design principles are applied to a new application of current interest -- a 1-watt Stirling-cycle cooler operating at 60K from a 280K heat sink. The modest cold-side temperature (60K) for this design requires that temperature dependent material properties be used, but is not so cold that it rules out simple calculational procedures.

In the subsections that follow, the heat-switch design process is divided into four elements:

1) Establishing the design requirements of the switch -- in particular, the maximum allowable thermal resistance of the switch in the 'on' state, and the minimum allowable thermal resistance in the 'off' state.

2) Designing the switch diameter and gas-gap area to achieve the required 'on' resistance, while avoiding

thermal contact between the fins under conditions with severe thermal gradients.

3) Selecting the support tube thickness, switch radiative properties, and 'off'-state vacuum levels to minimize parasitic heating of the cold side in the 'off' state.

4) Designing the gas charging/venting system to achieve the required switching pressures.

Each of these steps is detailed below.

4.1 ESTABLISHING DESIGN REQUIREMENTS

The first step in the design process is to establish the heat-switch design requirements, namely the maximum allowable 'on' resistance and minimum allowable 'off' resistance. This process is generally interactive with the design process -- beginning with comfortable starting values, then backing off or tightening up, depending on the complexity and producibility of the resulting heat-switch design.

As a reasonable starting point, it is useful to make the thermal losses associated with both the 'on' heat switch, and the 'off' heat switch, equal to a tolerable fraction -- say 10% -- of the cooling power of the cooler.

For the 'on' heat switch, this implies selecting an allowable temperature drop across the switch that corresponds to a 10% loss in cooler output cooling power. For our 1-watt/60K Stirling-cooler example we shall assume that a 10% loss corresponds to a 2K temperature drop; this gives the allowable 'on' resistance:

$$R_N = 2\ K/(1\ watt) = 2\ K/W \qquad (4.1)$$

Before setting the allowable heat-switch 'off' resistance, it is important to note that the thermal resistance of the 'off' cooler is likely to be a significant fraction of that of the 'off' heat switch; it is therefore important to examine the total thermal network representing the heat switches, the coolers, and the thermal load.

A representative network is illustrated in Figure 4-1. Here T_R is the heat rejection temperature of the cooler, and R_R represents the thermal resistance between the cold end and the heat-rejection end of the nonoperating refrigerator. R_N and R_F are the 'on' and 'off' resistances of the heat switch, respectively.

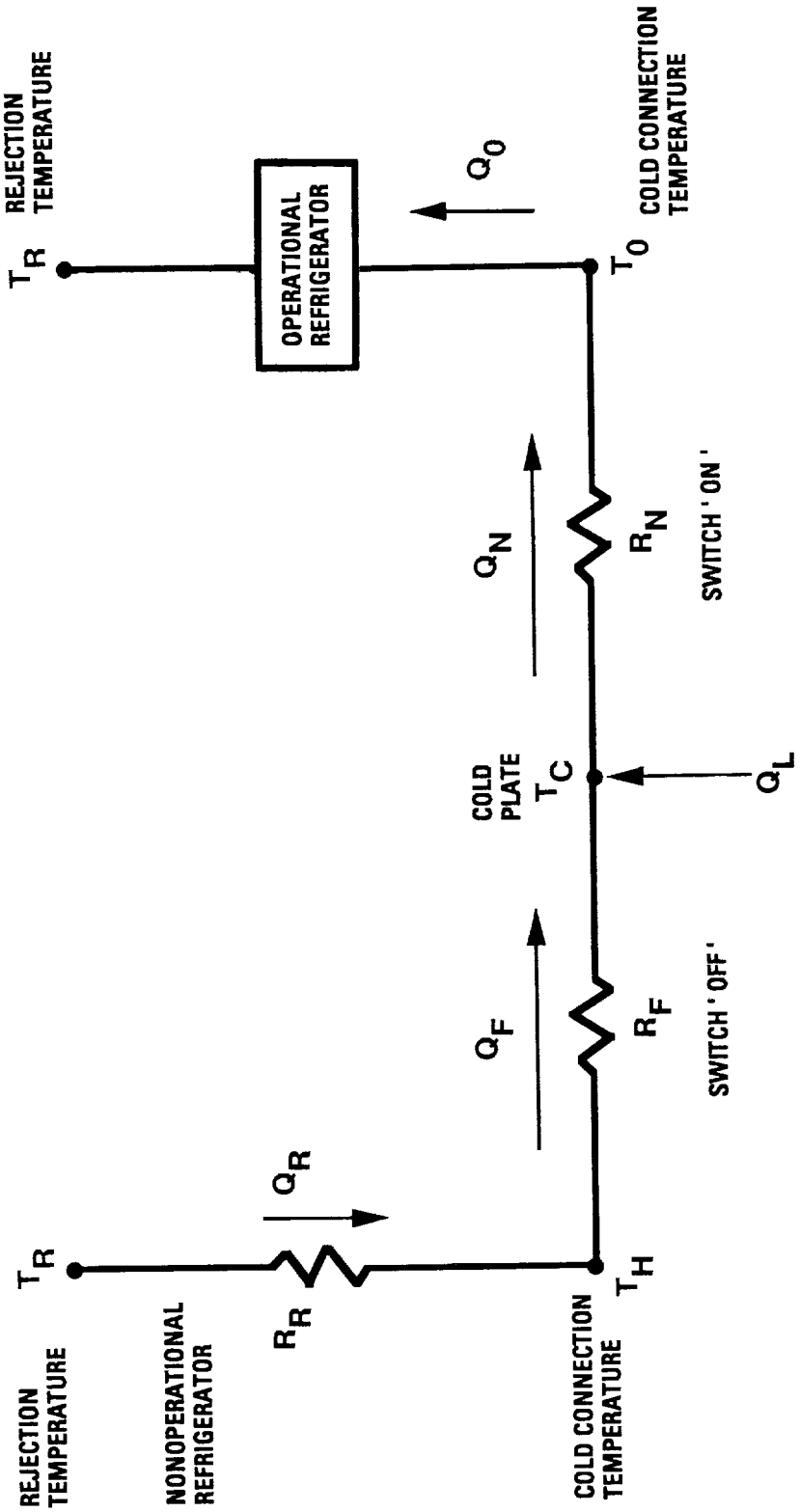

Figure 4-1. Network Model of the Heat-switch/Cooler/Load Interface

By making flow balances between the various nodes of the network, it is possible to derive four equations that are useful for examining the implications of various heat-switch 'on' and 'off' resistances in terms of the overall cooling system operation:

$$Q_R = Q_F = (T_R - T_C)/(R_R + R_F) \quad (4.2)$$

$$R_F = (T_R - T_C)/Q_R - R_R \quad (4.3)$$

$$T_H = Q_R R_F + T_C = (R_F T_R + R_R T_C)/(R_R + R_F) \quad (4.4)$$

$$T_O = T_C - Q_O R_N \quad (4.5)$$

where

T_C = cold load temperature, (e.g. 60K)
T_O = temperature of the operational refrigerator (K)
T_H = temperature of the nonoperational refrigerator (K)
T_R = heat rejection temperature, (e.g. 280K)
Q_R = parasitic load through 'off' heat-switch/refrig. (watts)
Q_L = cold load (watts)
Q_O = total refrigeration load = $Q_L + Q_R$ (watts)
R_R = thermal resistance of the 'off' refrigerator (K/watt)
R_F = thermal resistance of the 'off' heat switch (K/watt)
R_N = thermal resistance of the 'on' heat switch (K/watt)

To obtain the requirement for the 'off' heat switch we use Eq.(4.3), with the allowable parasitic conduction (Q_R) set equal to 10% of the cooling load (Q_L), assuming the temperature drop across the heat switch/cooler combination is the difference between the cryogenic load temperature (T_C) and the cooler heat-rejection temperature (T_R).

For our example, we assume that the Stirling-cycle cooler has a measured nonoperating thermal conductive loss of 0.5 watts from the cold finger at 60K to the heat rejection surfaces at 280K. For comparison, the parasitic heat conduction of the well known Oxford Stirling-cycle cooler is also approximately 0.5 watts (Reference 6).

For this level of parasitics, the thermal resistance (R_R) of the nonoperating cooler is given by:

$$R_R = (280K - 60K)/(0.5 \text{ watt}) = 440 \text{ K/W} \quad (4.6)$$

Thus, using Eq.(4.3), the required resistance of the 'off' heat switch is:

$$R_F = \frac{T_R - T_C}{Q_R} - R_R = \frac{(280K - 60K)}{0.1 watts} - 440 = 1760\ K/W \qquad (4.7)$$

Using this value together with the assumed heat-switch 'on' resistance (R_N) of 2 K/W (from Eq.4.1) allows the effect of various ratios of heat-switch 'off' to 'on' resistance to be analyzed. Figure 4-2 presents the computed results for two key parameters: the total refrigerator heat load (Q_0), and the heat-switch hot-side temperature (T_H). It is clear from this figure that the range of useful heat-switch ratios is from 1000 to 10,000, and that for these ratios, the heat-switch hot-side temperature is close to the heat rejection temperature (T_R).

4.2 DESIGNING FOR THE 'ON' RESISTANCE

The principal parameters governing the heat-switch 'on' resistance are the total gas-gap area and spacing, and the fin conductance.

Fin Conductance Losses

In general, in an optimum heat-switch design, temperature drops down the fins should represent a small fraction, say 20%, of the total heat-switch conductive losses, i.e., 20% of the allocated 'on'-mode temperature drop across the switch. For small thermal gradients down the fins, the temperature drop down the length (L_f) of the fins can be accurately approximated as:

$$\Delta T_f = \frac{Q_f}{2 k_c} \left[\frac{L_f}{(wt)} - \frac{1}{(w+t)} \right] \approx \frac{Q_f\ L_f}{2 k_c\ A_f} \qquad (4.8)$$

where

ΔT_f = temperature drop down fin (K)
Q_f = heat conduction per fin (watts)
k_c = thermal conductivity of copper @ T_C (watts/cm-K)
w = width of fin (cm)
t = thickness of fin (cm)
L_f = length of fin (cm)
A_f = cross-sectional area of each fin (cm^2)

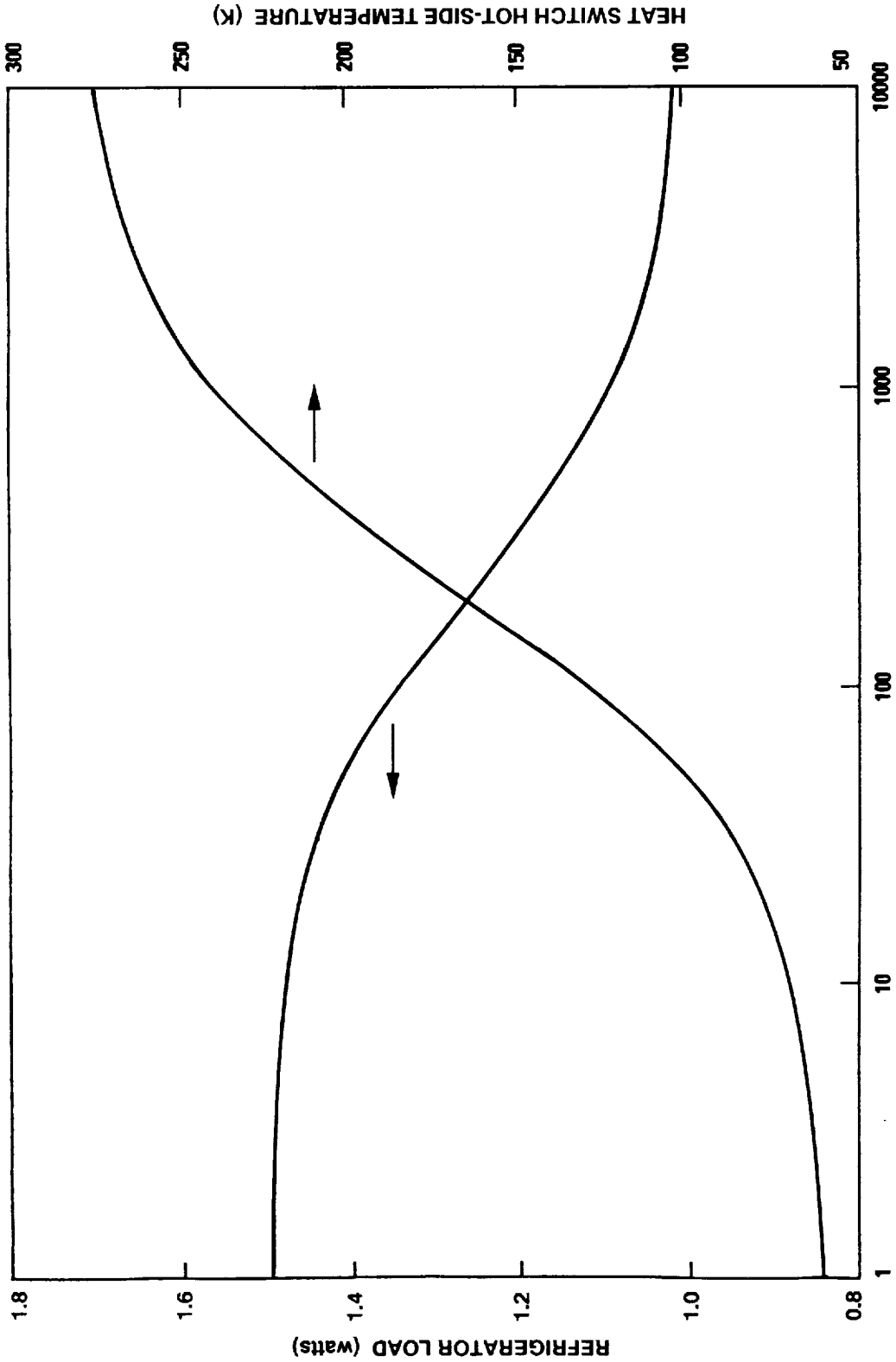

Figure 4-2. Effect of Heat-switch on/off Resistance Ratio on Total Refrigeration Load and Heat-switch Hot-side Temperature (R_N=2K/W)

For initial heat-switch sizing, it is useful to use Eq.(4.8) to establish an estimate of the heat-switch diameter (D) required to achieve the total allocated temperature drop down the heat switch copper body including the fins; i.e. $\Delta T_b = \Delta T_f + \Delta T_e$, where ΔT_e is the total combined temperature drop for both solid ends of the heat switch.

For this we assume that the total cross-sectional area of the fins is made the same on both sides of the switch, and therefore the fins on each side represent approximately 50% of the total cross-sectional area of the switch, i.e. total $A_f = A/2$. Noting that the total fin heat conduction (total Q_f) is the same as the total heat-switch heat conduction (Q), Eq.(4.8) gives:

$$\Delta T_b = \frac{Q\, L_f}{2\, k_c (A/2)} + \frac{Q\, L_e}{k_c\, A} = \frac{Q\, L}{k_c\, A}$$

Therefore,

$$D = (4A/\pi)^{1/2} = \left[\frac{4\,Q\,L}{\pi\, k_c\, \Delta T_b}\right]^{1/2} = \left[\frac{4\,L}{\pi\, k_c\, R_b}\right]^{1/2} \qquad (4.9)$$

where

D	=	heat switch diameter (cm)
Q	=	total heat switch power transmission (watts)
L	=	total heat switch length (including ends)(cm)
L_f	=	length of fins (cm)
L_e	=	combined length of heat-switch ends (cm)
ΔT_b	=	'on'-mode ΔT allocation for switch body (K)
k_c	=	thermal conductivity of copper at T_c (watts/cm-K)
R_b	=	total thermal resistance allocation for fin/body conduction (K/watt)

Although Eq.(4.9) was derived from the fin equation, it is identical to that for a solid copper rod of diameter D and length L. Thus, in the 'on' mode the switch merely acts as two resistances in series: that of a copper rod the diameter and length of the heat switch, plus that of the gas gap.

To demonstrate Eq.(4.9), consider the problem of designing a heat switch for our example Stirling cooler. A key consideration is selecting the right copper, since at cryogenic temperatures, its thermal conductivity is very sensitive to the level of impurities and work hardening. Figure 4-3 highlights this sensitivity, but suggests that the difference is small for

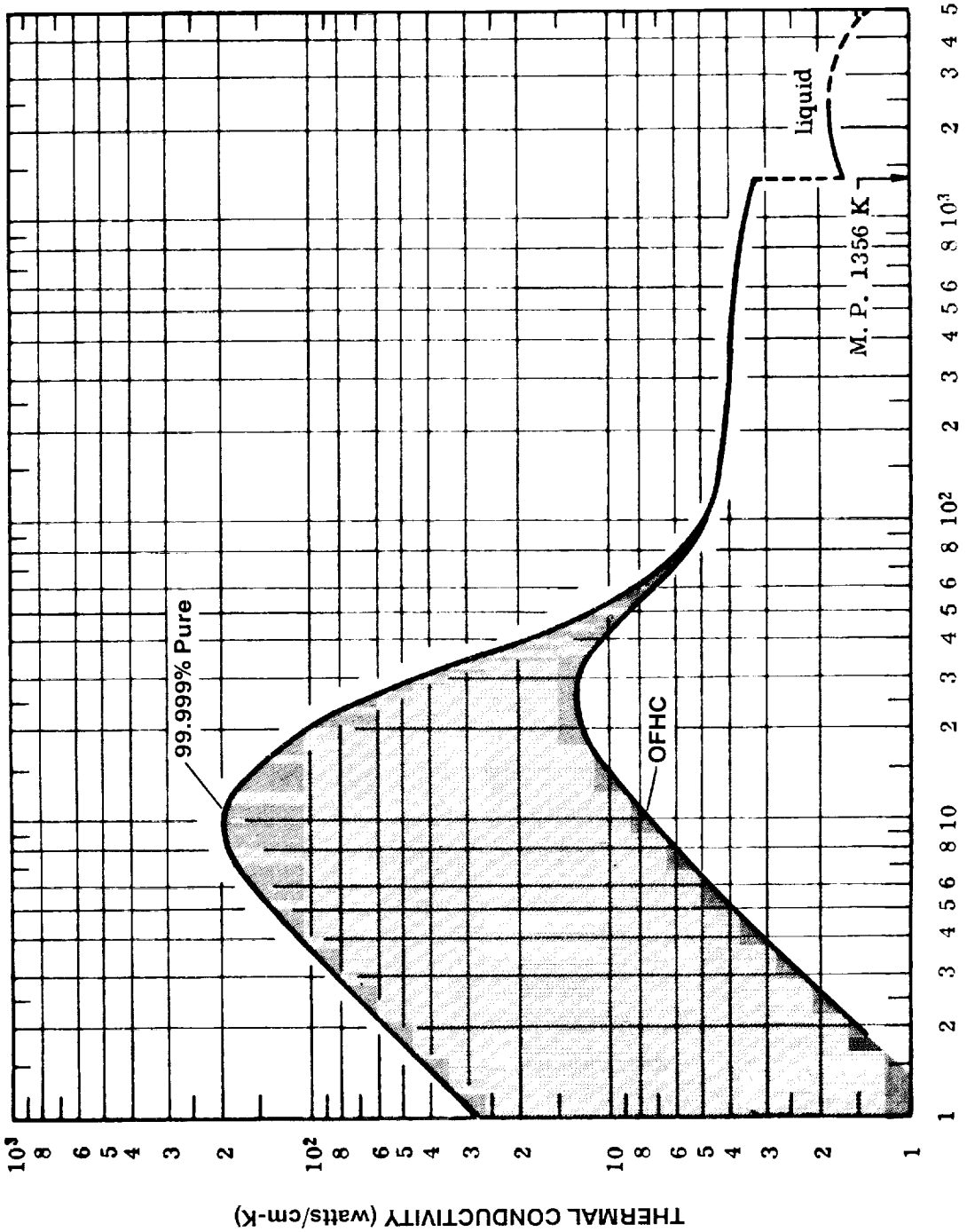

Figure 4-3. Thermal Conductivity of High Purity Coppers as a Function of Temperature

temperatures above 60K; we therefore select a common OFHC copper with a conductivity around 7 watts/cm-K at 60K. Next, we select a trial length of 4 cm for the heat switch -- a balance between shortening the switch to reduce the 'on' resistance, and lengthening it to increase the 'off' resistance. A 20% 'on'-resistance allocation to the copper/fins gives $R_b = 0.2 \times 2 = 0.4$K/watt, so that Eq.(4.9) yields:

$$D = \left(\frac{4 \times 4 \text{ cm}}{3.14 \times 7 \times 0.4} \right)^{\frac{1}{2}} = 1.35 \text{ cm} \qquad (4.10)$$

Gaseous Conduction Losses

The second half of the 'on'-conduction calculation relates to sizing the gas-gap area to limit the temperature differential across the gas gap. For this calculation we assume that the gas in the gap is pressurized sufficiently to insure that it is in the continuum regime, i.e., above the corresponding upper line in Figure 4-4 (for the derivation of this plot see Reference 1). For example, with hydrogen and a 0.005 cm gap spacing, the minimum required pressure is approximately 30 torr.

Once in the continuum regime, the conductivity (k_g) of the gas in the gap is solely a function of its temperature, as shown in Figure 4-5. The thermal resistance (R_g) across the gap (g) is therefore given as:

$$R_g = \frac{g}{A_g k_g} \qquad (4.11)$$

so that the required total gas-gap area (A_g) is given by:

$$A_g = \frac{g}{R_g k_g} \qquad (4.12)$$

where

A_g = total gas-gap area in heat switch (cm^2)
g = gap spacing (typically 0.005 cm)
k_g = conductivity of gas at 'on'-mode temperature (watts/cm-K)
R_g = allocation for gas-gap conduction resistance (K/watt)

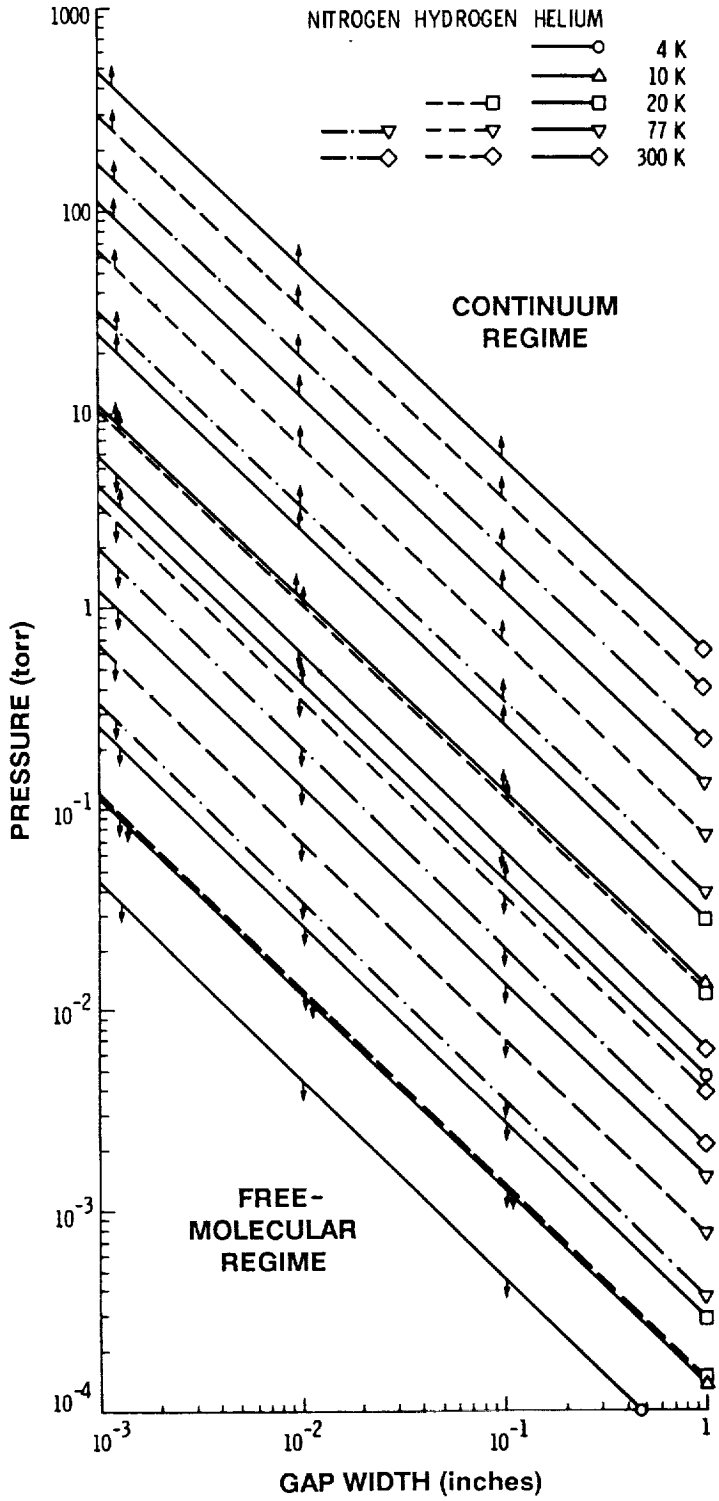

Figure 4-4. Gas Pressure Bounds for the Continuum and Free-Molecular Conduction Regimes for N_2, H_2 and He

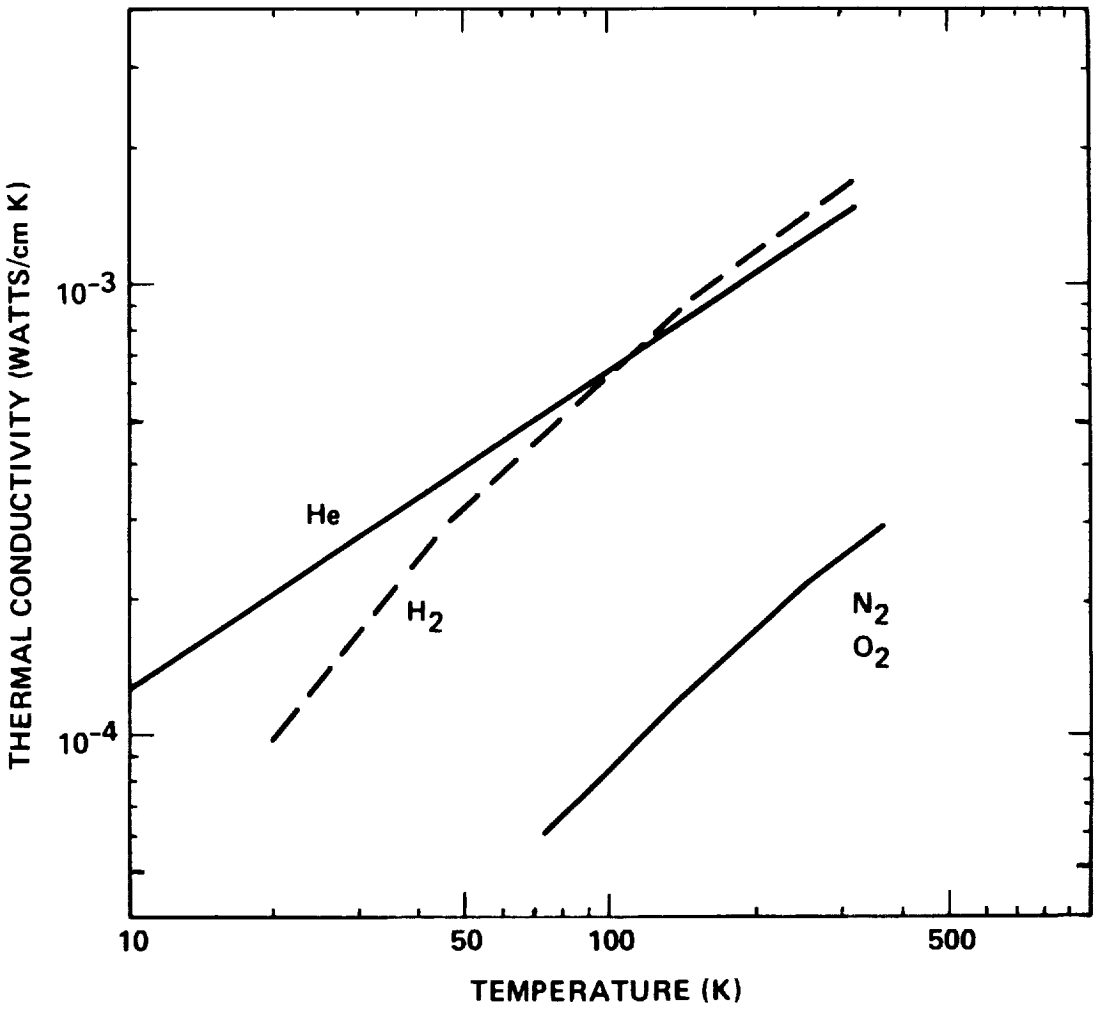

Figure 4-5. Thermal Conductivity versus Temperature for Various Gases in the Continuum Regime

For our Stirling-cooler heat switch we select hydrogen gas to achieve both a high conductivity (0.00038 watts/cm-K from Figure 4-5), and the ability to achieve low (10^{-3} torr) pressures with a charcoal sorption pump at 60K (discussed later in Section 4.5). Combining this conductivity with our gas-gap resistance allocation of $R_g = R_N - R_b = 1.6$ K/W (Eqs. 4.1 and 4.10), gives:

$$A_g = (0.005 \text{ cm} / (1.6 \times 0.00038) = 8.22 \text{ cm}^2 \qquad (4.13)$$

4.3 SWITCH GEOMETRY SELECTION

Once the switch diameter and gas-gap area have been defined using Eqs.(4.9) and (4.12), the next step is to select an initial switch configuration that both satisfies these constraints, and addresses important manufacturing and operational tolerance issues. Three of the most important of these issues include:

1) Selecting a symmetrical fin arrangement so as to prevent possible warping of the heat switch during conditions of large temperature differences between the switch halves.

2) Minimizing the radial distance from the switch centerline to the farthest gas gap to avoid gap closure due to differential expansion of the switch halves during 'off' conditions.

3) Maintaining sufficient axial clearance between the ends of the fins and the slot bottoms of the mating half to avoid fin bottoming.

For our example problem, the diameter derived in Eq.(4.10) and the gas-gap area derived in Eq.(4.13) can both be satisfied by the fin configuration shown in Figure 4-6. This configuration has a number of important attributes:

1) It is relatively easy to machine.

2) It is symmetrical so as to avoid any warping in the 'off' mode.

3) The radial distance from the switch centerline to the farthest gas gap is quite small (0.27cm).

Two important dimensions that must be confirmed are the radial and axial fin clearances during 'off' conditions where large temperature differences exist between the switch halves.

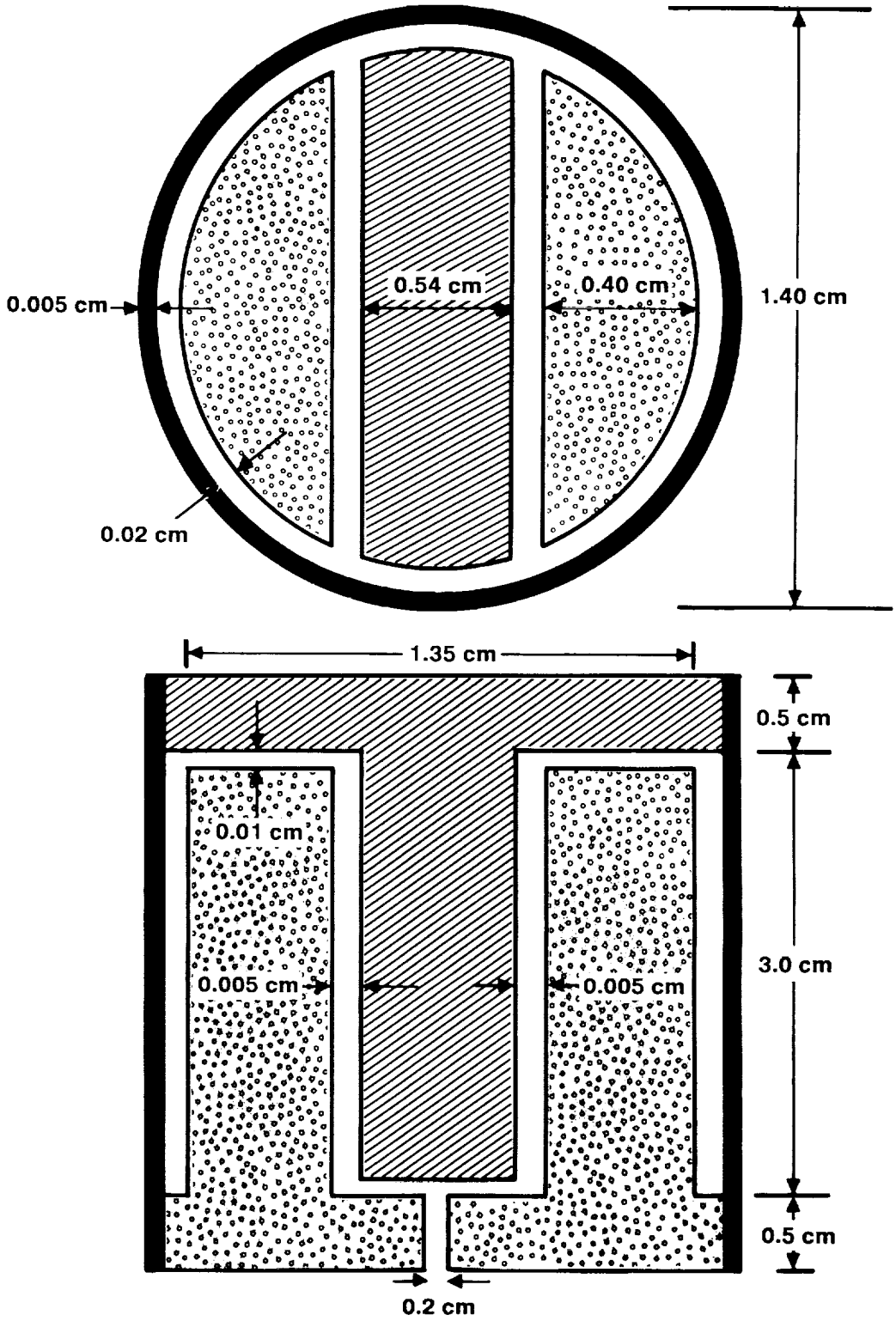

Figure 4-6. Trial Heat-switch Configuration for Example 1-watt / 60K Stirling Cooler

Axial Clearance Calculation

Reduction in the hot-fin axial or end clearance occurs during 'off' conditions when large temperature differentials develop across the switch. Under these conditions the outer support tube shrinks relative to the hot fins, thereby closing the axial gap between the tips of the hot fins and the bottoms of the cold-fin slots. Because the hot fins are essentially isothermal, their change in length from room temperature is readily computed as:

$$\Delta L_f = \alpha_c L_f (300 - T_H) \tag{4.14}$$

where

ΔL_f = change in hot-fin length (cm)
α_c = average CTE of copper between 300K and T_H (m/m-K)
L_f = length of the fins plus hot base of switch (cm)
T_H = heat-switch hot-side temperature (K)

Because the support tube will generally have a large, often non-linear temperature variation, computing its change in length may require a numerical solution that divides the tube length into 5 or more sections. To obtain a quick approximation of the tube shrinkage it is useful to simply use the average tube temperature and the average CTE of the tube material over the range of applicable temperatures. Thus:

$$\Delta L_t \approx \alpha_t L_t (300 - (T_H + T_C)/2) \tag{4.15}$$

where

ΔL_t = change (shrinkage) in support tube length (cm)
α_t = ave. CTE of support tube between 300K and T_C (m/m-K)
T_C = heat switch cold-side temperature (K)
L_t = unsupported length of support tube (cm)

Typical CTE data for copper, stainless steel, and titanium are provided as a function of temperature in Figure 4-7.

Using these data in our example gives:

$$\Delta L_f = (16.3 \times 10^{-6})(3\,\text{cm})(300\text{K} - 280\text{K}) = 0.0009\ \text{cm} \tag{4.16}$$

$$\Delta L_t = (8 \times 10^{-6})(3\,\text{cm})(300\text{K} - 170\text{K}) = 0.0031\ \text{cm} \tag{4.17}$$

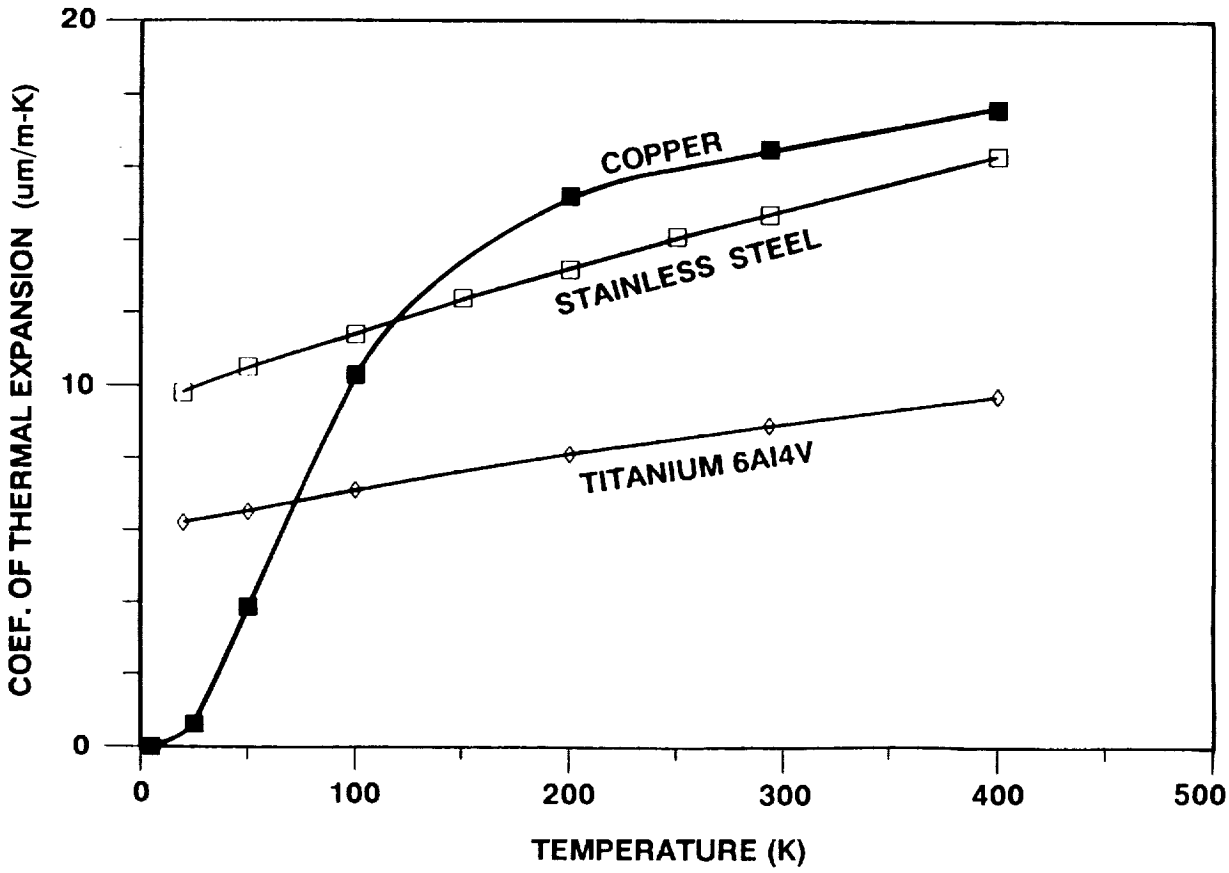

Figure 4-7. Coefficient of Thermal Expansion for Copper, 300 Series Stainless Steel and Titanium 6A14V

The net shrinkage of the end gap is thus:

$$\Delta L_g = L_t - L_f = (0.0031 - 0.0009) = 0.0022 \text{ cm} \qquad (4.18)$$

This is easily accommodated by the 0.010 cm gap proposed in Figure 4-6.

Radial Clearance Calculation

Reduction in the fin radial or side clearance also occurs during 'off' conditions when large temperature differentials develop across the switch. Under these conditions the cold half of the switch shrinks relative to the hot half. The net reduction in the thickness of the gas gaps is thus given by:

$$\Delta g = \alpha_c r (T_H - T_C) \qquad (4.19)$$

where

Δg = gas-gap thickness reduction (cm)
r = radial distance to the gas gap from the heat-switch centerline (cm)
α_c = average CTE of copper between T_C and T_H (m/m-K)
T_H = hot-side temperature (K)
T_C = cold-side temperature (K)

For our example, Eq.(4.19) gives:

$$\Delta g = (12 \times 10^{-6})(0.27 \text{ cm})(280\text{K} - 60\text{K}) = 0.0007 \text{ cm} \qquad (4.20)$$

This is easily accommodated by the 0.005 cm gap proposed in Figure 4-6.

4.4 ASSESSING THE 'OFF'-MODE PERFORMANCE

The principal parameters affecting the 'off'-mode performance of the heat switch are the thermal conductance down the support tube, the radiative exchange between the fins, and the 'off'-mode conductance of the evacuated gas in the gas gap, i.e.:

$$K_f = K_t + K_r + K_g$$

To meet the stipulation of Eq.(4.7) that $R_F \geq 1760$ K/W requires that the sum of these conductances be below the limiting value defined by:

$$K_F = 1/R_F \leq 1/1760 \leq 0.568 \text{ mW/K} \tag{4.21}$$

Thermal Conductance Down the Support Tube (K_t)

The 'off'-mode thermal conductance (K_t) down the support tube is well approximated by the conduction equation:

$$K_t = \frac{k_t A}{L_t} = \frac{\pi k_t D t}{L_t} \tag{4.22}$$

where

K_t = Conductance of the support tube (watts/K)
k_t = average thermal conductivity of support tube over the temperature range T_H to T_C, (watts/cm-K)
D = tube diameter (cm)
t = tube thickness (cm)
L_t = tube unsupported length (cm)
T_C = heat switch cold-side temperature (K)
T_H = heat switch hot-side temperature (K)

Figure 4-8 provides representative conductivity data for two materials: stainless steel and titanium. For our example, we select a 0.005 cm thick titanium support tube with a 3-cm long unsupported length. Thus:

$$K_t = \frac{3.14 \times 0.125 \times 1.40 \times .005}{3} = 0.916 \text{ mW/K} \tag{4.23}$$

This value is somewhat greater than the allocated 'off'-mode conductance in Eq.(4.21) for our heat-switch design, and suggests a need to lower the conductance of the support tube if possible. Because it is difficult to manufacture and assemble tubes with wall thicknesses much less than 0.005 cm (0.002 inch), one is faced with either reducing the diameter or increasing the tube length. Unfortunately, reducing the diameter has an immediate detrimental impact on the switch's 'on' resistance, which tends to vary with the square of the diameter. As a result, any attempt to reduce the diameter leads to a runaway increase in the 'on' resistance.

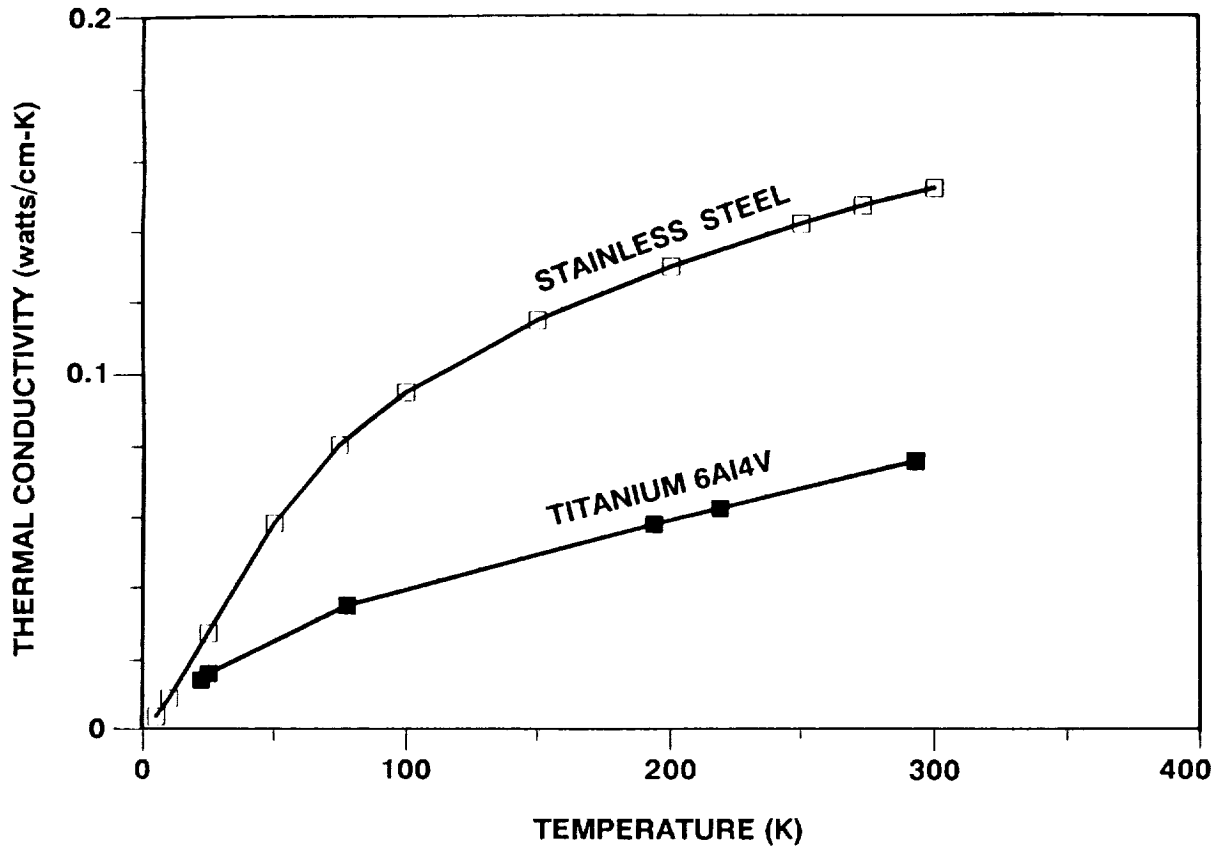

Figure 4-8. Thermal Conductivity Data for 300 Series Stainless Steel and Titanium 6A14V

Increasing the tube resistance by increasing its length is the other alternative. If this is done by increasing the total switch length, this will lead to a linear increase in the copper conductivity losses (ΔT_b) in the 'on' mode, and will increase the difficulty of alignment and assembly of the switch halves.

An interesting alternative is to use the folded-tube design illustrated in Figure 4-9; this design nearly triples the outer wall length while leaving the heat-switch conductive elements unaffected. This reduces the conductive losses down the support tube to about 0.3 mW/K -- well within the allocation. Although this concept has been used previously at JPL, the alignment and assembly issues associated with this application have not been examined, and would have to be developed and proven.

Radiative Heat Transfer Across the Gap

Because of the large temperature differential across the switch in the 'off' mode, radiative exchange between the hot and cold fins may be an important consideration. For closely spaced parallel fins the radiative heat transfer is given by:

$$Q_r = \frac{\sigma A_g (T_H^4 - T_C^4)}{(1/\epsilon_H + 1/\epsilon_C - 1)} \qquad (4.24)$$

$$\approx \sigma A_g \epsilon T_H^4 /2 \quad \text{for } T_H >> T_C \text{ and } \epsilon << 1 \qquad (4.25)$$

where

Q_r = radiative heat transfer across 'off' switch (watts)
T_H = temperature of hot side (K)
T_C = temperature of cold side (K)
ϵ = emissivity of fin surfaces
A_g = total gas-gap area including switch ends (cm^2)
σ = Stefan-Boltzmann Constant (5.67×10^{-12} watts/$cm^2 K^4$)

For our example heat switch we assume gold-plated fin surfaces with an average emissivity of 0.02. Thus:

$$Q_r \approx (5.67)\times(10\,cm^2)\times(0.02) \times \left[\frac{280}{1000}\right]^4 /2 = 0.003 \text{ watts} \qquad (4.26)$$

Thus, radiative heat transfer is negligible in this design.

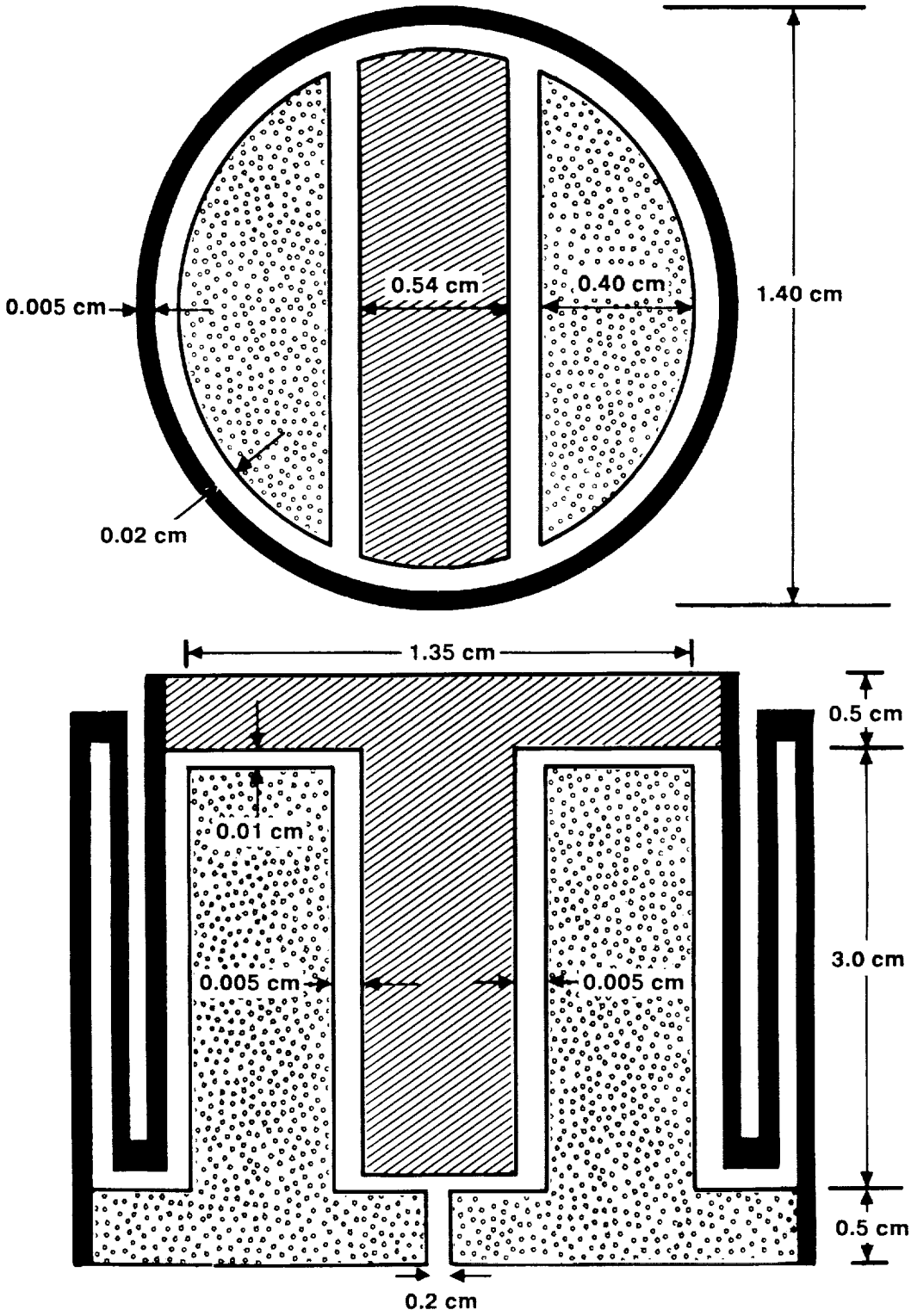

Figure 4-9. Modified Heat-switch Configuration for Reduced Support-tube Conductance

Heat Leakage by Gaseous Conduction (K_g)

The fundamental operating principle of the gas-gap heat switch is to reduce the gaseous conduction between the switch halves in the 'off' mode by reducing the gas pressure. At very low gas pressures, the thermal conductivity of the gas is determined by the relationship between the gap spacing and the mean free path length between gas-molecule collisions. When the gap is small compared to the mean free path length, the gas is said to be in the free-molecular regime, and the thermal conductance becomes independent of the gap spacing and directly proportional to the gas pressure. In this regime the thermal conductance across the gap is given by:

$$K_g = \kappa A_g p \tag{4.27}$$

where

K_g = Gaseous conductance across the gap (watts/K)
κ = free molecular gas conductance (watts/cm^2 K torr)
A_g = total gas-gap area (cm^2)
p = pressure of the gas in the gas gap measured by a remote pressure gage at room temperature (torr)

The free molecular gas conductance (κ) is a complex function of the physical properties of the gas-gap gas, and the ability of the gas molecules striking the switch surfaces to achieve the temperature of the surface; this later characteristic, referred to as the gases accommodation coefficient, varies from 0.3 to 1.0 depending on the temperature of the surface that the gas contacts. For closely spaced surfaces, such as the gas gap walls, κ is given by (References 7 and 8):

$$\kappa = \frac{\gamma+1}{\gamma-1}\left(\frac{cR}{8\pi MT}\right)^{\frac{1}{2}} \Big/ \left(\frac{1}{a_H} + \frac{1}{a_C} - 1\right) \tag{4.28}$$

where

κ = free-molecular gas conductance (watts/cm^2 K torr)
γ = specific-heat ratio of gas-gap gas ($\approx$1.40)
M = gas molecular weight (grams/mole)
R = universal gas constant (8.48×10^4 g-cm/mole-K)
T = temperature of pressure gage (300 K)
a_H = accommodation coefficient of gas at temperature T_H
a_C = accommodation coefficient of gas at temperature T_C
c = unit conversion factor (1.744×10^{-5} watts^2/cm^5-torr^2)

Figure 4-10 provides values of κ for He, H_2, and N_2 as a function of cold wall temperature (T_c) for hot wall temperatures in the 250 to 300 K temperature range.

In our example heat switch, hydrogen is proposed as the working gas. Using Eq.(4.27) we obtain the following relationship for the gaseous conductance as a function of the quality of vacuum achieved in the gas gap:

$$K_g = (0.014)(10\,cm^2)p = 140p \ (mW/K) \qquad (4.29)$$

$$= 14.00 \ mW/K \text{ for } p = 10^{-1} \text{ torr}$$
$$= 1.400 \ mW/K \text{ for } p = 10^{-2} \text{ torr}$$
$$= 0.140 \ mW/K \text{ for } p = 10^{-3} \text{ torr}$$
$$= 0.014 \ mW/K \text{ for } p = 10^{-4} \text{ torr}$$

These data confirm that the gaseous conduction losses are negligible for gas-gap vacuums better than 10^{-3} torr.

4.5 SORPTION PUMP DESIGN

As a last step in the design process, the sorption pump must be designed to provide the pressure and vacuum required for operation of the switch. The pump will normally be connected to only one side of the switch so as to minimize heat-conduction parasitics between the switch halves in the 'off' mode; the cold side is often preferred, so as to minimize parasitics to the pump when the pump must be cooled to cryogenic temperatures to achieve the required 'off'-mode vacuum. Because the sorption bed must be heated to provide gas for the 'on' mode, it is critical that it be thermally well isolated from the switch body.

One possible means of heating and cooling the sorption pump is to attach it to the cold finger of the neighboring redundant cooler; this has the advantage of automatically providing the correct heating/cooling polarity to the heat switch. The only caveat is that the redundant cooler must be able to carry the full parasitics of the nonoperational cooler down to the temperature required for the heat switch to open. This sorption pump temperature required to pull a significant vacuum (below 10^{-3} torr) is thus a critical design parameter. A second design driver is the upper temperature that must be reached to provide the required gas quantity and pressure for switch conduction; as noted earlier in Figure 4-4, this pressure is normally in the range of 10 to 100 torr.

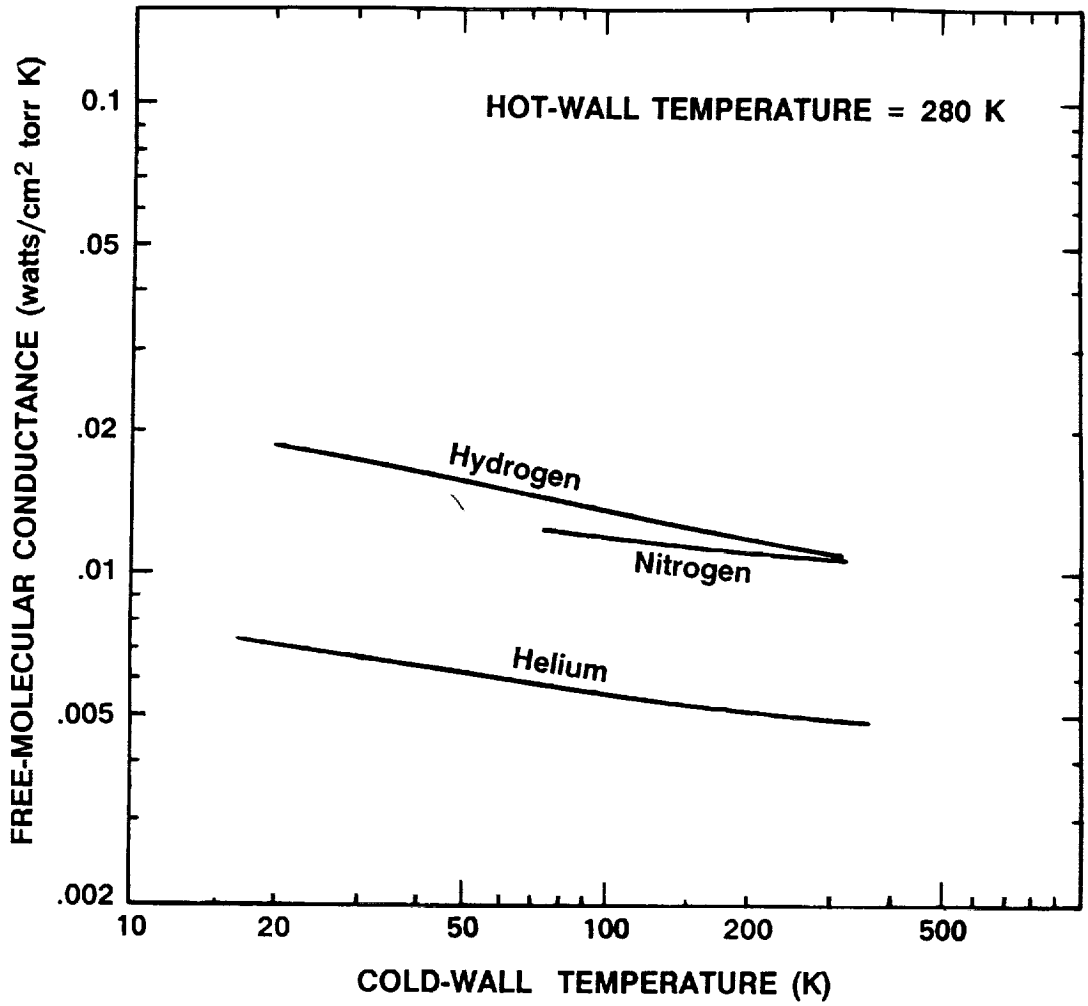

Figure 4-10. Conductance of Different Gases in the Free-molecular Conductance Regime

Figure 4-11 presents representative isotherm data relating the amount of two gases, helium and hydrogen, adsorbed by PCB charcoal as a function of temperature and pressure. Because charcoal is a physical adsorption medium, similar data are available in the literature for a broad variety of additional gases. However, the high thermal conductivity of helium and hydrogen (see Figure 4-5) makes them particularly good choices.

For hydrogen, an alternative to physical sorption on charcoal is the use of chemisorption hydrides; however, a disadvantage of these is the issue of whether the pump will sufficiently extract possible outgassing gases that may be other than the chemisorbed gas. The advantage of the chemisorbers is that they typically sorb at much higher temperatures.

Based on the data of Figure 4-11 we have selected hydrogen gas with a charcoal pump for our example design; this should provide a pumping capacity of approximately 10cc STP of hydrogen per gram of charcoal at 60K and 10^{-3} torr. If the volume of gas in the heat switch and connecting tubing is 2cc at 60K, this will require about 1.3cc of hydrogen at STP, or 1.3/10 = 0.13 gram of charcoal.

A conservative adsorption pump design would involve 0.5 gram of charcoal, which occupies 0.28 cm^3 and is equivalent to a rod 4 mm in diameter by 2 cm long. The heat capacity of a suitable copper container with 0.25-mm thickness and weighing 0.6 grm is 0.24 J/K. The heat capacity of the 0.5 gm of charcoal is 0.34 J/K. The heat adsorption for hydrogen is 0.7 J (based on 5000 J per g-mole for the heat of adsorption). The heat input to the pump is 1.76 W during a 30-second turn-on period, which will raise the temperature from 60K to 150K.

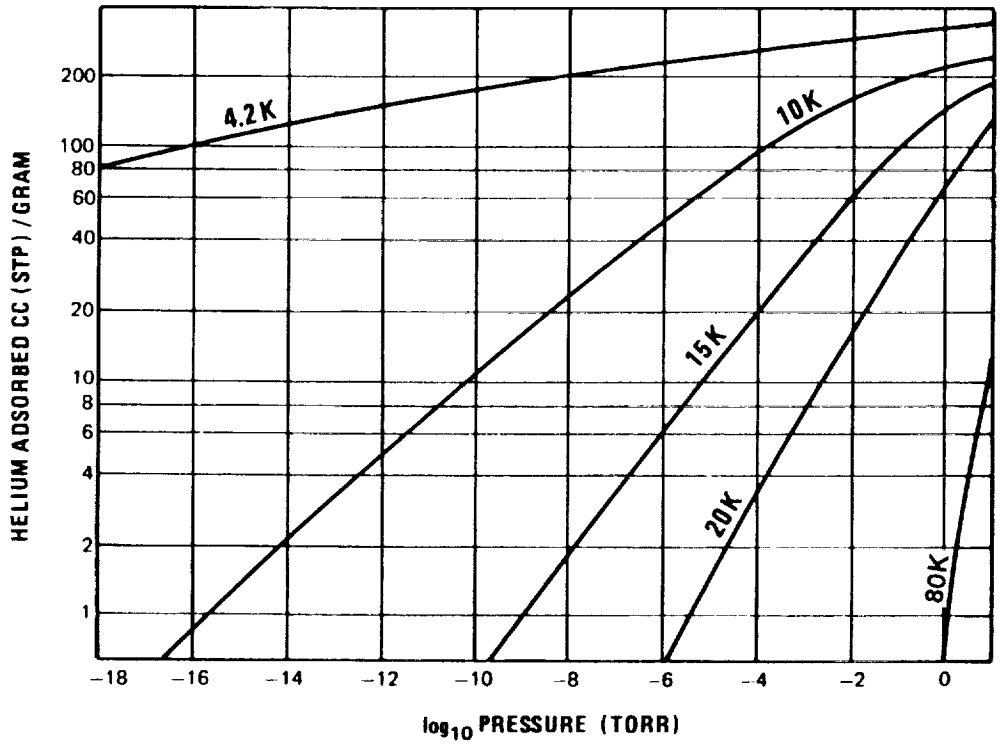

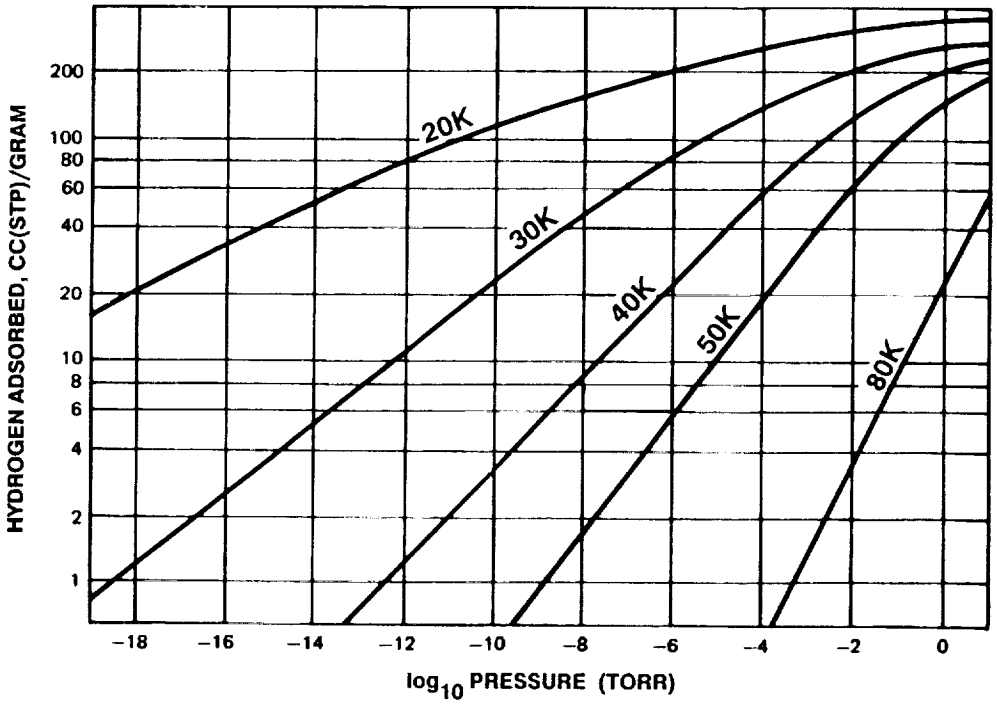

Figure 4-11. Sorption Isotherm Data for Helium and Hydrogen on PCB Charcoal

SECTION 5

SUMMARY

Over the course of the Phase I and Phase II contract activities, a cryogenic gas-gap heat switch concept for isolating redundant cryocoolers has been carried from initial concept through successful engineering model testing. In the process, the design has been thoroughly documented, and computer programs have been developed to provide the technology base required for future flight designs. An extensive test program has both verified the excellent performance of the heat switch, and highlighted minor deficiencies. These deficiencies, associated with heat-switch shorting during conditions of large temperature differentials across the switch halves, have been thoroughly analyzed and understood. Means are described for eliminating these shortcomings in future designs. Lastly, the overall process of designing cryogenic gas-gap heat switches has been concisely summarized, and demonstrated for a 1-watt/60K Stirling-cooler application.

SECTION 6

REFERENCES

1. C. K. Chan, "Gas Adsorption/Absorption Heat Switch: Final Report of Phase I," JPL Publication 87-7, Jet Propulsion Laboratory, Pasadena, CA, July 15, 1987.

2. C. K. Chan, "Self-Actuated Heat Switches for Redundant Cryocoolers," Proceedings of the Second Interagency Meeting on Cryocoolers, David Taylor Research Center, Annapolis, MD, pp. 217-226, 1986.

3. "Self-Actuating Heat Switches for Redundant Refrigeration Systems," U. S. Patent 4,771,823, September 20, 1988.

4. A. M. Lehtinen, "Cryocooler Subsystem Integration," AFWAL-TR-87-3054, Wright Patterson Air Force Base, Ohio, September 11, 1987.

5. C. A. Lewis, "Long Life Stirling Cycle Coolers for Applications in the 60 - 110K Range: Vibration Characterization and Thermal Switch Development," SAE Paper 891496, Society of Automotive Engineers, Warrendale, PA, 1989.

6. A. H. Orlowska and G. Davey, "Measurement of Losses in Stirling Cycle Cooler," Cryogenics, Vol. 27, 1987, p. 645.

7. Barron, R., Cryogenic Systems, Second Edition, Oxford University Press, New York, N.Y., 1985.

8. Scott, R.B., Cryogenic Engineering, D. Van Nostrand Co., Inc., Princeton, N.J., 1959.

TECHNICAL REPORT STANDARD TITLE PAGE

1. Report No. JPL Pub. 90-38	2. Government Accession No.	3. Recipient's Catalog No.
4. Title and Subtitle Design and Application of Gas-Gap Heat Switches: Final Report of Phase II		5. Report Date March 15, 1990 6. Performing Organization Code
7. Author(s) C. K. Chan and R. G. Ross, Jr.		8. Performing Organization Report No.
9. Performing Organization Name and Address JET PROPULSION LABORATORY California Institute of Technology 4800 Oak Grove Drive Pasadena, California 91109		10. Work Unit No. 11. Contract or Grant No. NAS7-918 13. Type of Report and Period Covered Jpl Publication
12. Sponsoring Agency Name and Address NATIONAL AERONAUTICS AND SPACE ADMINISTRATION Washington, D.C. 20546		14. Sponsoring Agency Code RE/ PX-644-11-00-05-81

15. Supplementary Notes

16. Abstract

Gas-gap heat switches can serve as an effective means of thermally disconnecting a standby cryocooler when the primary (operating) cooler is connected and vice versa. This report describes the final phase of the development and test of a cryogenic gas-gap heat switch designed for loads ranging from 2 watts at 8K, to 100 watts at 80K. Achieved heat-switch on/off conductance ratios ranged from 11,000 at 8K to 2200 at 80K.

A particularly challenging element of heat-switch design is achieving satisfactory operation when large temperature differentials exist across the switch. A special series of tests and analyses was conducted and used in this Phase-II acitivity to evaluate the developed switches for temeprature differentials ranging up to 200K. Problems encountered at the maximum levels are described and analyzed, and means of avoiding the problems in the future are presented. The report concludes with a comprehensive summary of the overall heat-switch design methodology with special emphasis on lessons learned over the course of the 4-year development effort.

17. Key Words (Selected by Author(s))	18. Distribution Statement
Components Fluid Mechanics and Heat Transfer	Unclassified -- Unlimited

19. Security Classif. (of this report)	20. Security Classif. (of this page)	21. No. of Pages	22. Price
Unclassified	Unclassified	59	